UNIVERSIDADE DE LISBOA
FACULDADE DE CIÊNCIAS
DEPARTAMENTO DE GEOLOGIA

Flood risk assessment in climate change scenarios in the Algarve region

Linnea Dawo

Mestrado Bolonha em Geologia do Ambiente, Riscos Geológicos e Ordenamento do Território

Dissertação orientada por:
Fátima Cristina Gomes Ponte Lira
Luís Filipe Antunes Dias

2022

Acknowledgements

I would like to thank my supervisors Fátima Cristina Gomes Ponte Lira and Luís Filipe Antunes Dias for their help and guidance throughout this master thesis. Additionally, I would like to thank the municipality of Tavira for the information and data about the landcover in Tavira.

Abstract

Natural hazards are extreme events that endanger people and their belongings. One of the most dangerous in terms of economic damages and impacts on the society are floods. Through climate change it is likely that their frequency and intensity will increase in the future, which together with land use changes can increase the flood risk. In order to assess the risk emerging from floods, the European Union passed a Directive on the assessment and management of flood risk, that was implemented in Portuguese law. The assessment of flood risk is important to evaluate where the risk is too high and mitigation measurements need to be applied. This thesis aimed at producing hazard maps (flood extent, depth and velocity), danger, and risk maps for the city of Tavira in southern Portugal. The analysis used two return periods (T20 and T100) for the flood events and considered climate change scenarios for three future time periods (2011-2040, 2041-2071, 2071-2100). The assessment was performed using geoinformation systems. The risk was evaluated in terms of the economic, social, and environmental risk, whereby the economic risk was calculated as the annual average damage. Besides that, the absolute damage emerging from one single flood event was calculated. The economic risk was obtained using depth-damage curves and probability-damage curves. The social risk was calculated as the annual average affected population and the probability of social hot spots being affected. For the environmental risk, sources that might cause pollution were identified and the possible impacts on the National Park Rio Formosa were discussed. There is a definite increase in the intensity of the flood events from the T20-scenarios to the T100-scnearios, and also when propagating further in the future. The highest values regarding the flood depth, flood velocity, flood danger and risk can be found in near distance to the river Gilão (that runs through Tavira) and are decreasing with higher distances to it. A big part of the flood extent affects the salines in the southern part of the city.

Key words: flood risk analysis, flood risk assessment, climate change, depth-damage curve, risk maps

Resumo

Os riscos naturais são eventos extremos que colocam em risco as pessoas e seus pertences. Um dos mais perigosos em termos de danos económicos e impactos na sociedade são as inundações. Com as alterações climáticas é provável que a sua frequência e intensidade aumentem no futuro, o que, juntamente com alterações no uso da terra, pode aumentar o risco de inundações. Para avaliar o risco de inundação, a União Europeia aprovou uma Diretiva sobre a avaliação e gestão do risco de inundação, que foi implementada na lei portuguesa. A avaliação do risco de inundação é importante para avaliar onde este é muito alto e as medidas de mitigação que precisam de ser aplicadas. Esta tese teve como objetivo produzir mapas de suscetibilidade (extensão, profundidade e velocidade de cheias), mapas de perigosidade e risco para a cidade de Tavira no sul de Portugal. A análise utilizou dois períodos de retorno (T20 e T100) para os eventos de inundação e considerou cenários de alterações climáticas para três períodos futuros (2011-2040, 2041-2071, 2071-2100). A avaliação foi realizada por meio de sistemas de geoinformação. O risco foi avaliado em termos de risco económico, social e ambiental, sendo o risco económico calculado como o dano médio anual. Além disso, foram calculados os danos absolutos decorrentes de um único evento de inundação. O risco económico foi obtido por meio de curvas profundidade-dano e curvas de probabilidade-dano. O risco social foi calculado como a média anual da população afetada e a probabilidade de focos sociais serem afetados. Para o risco ambiental, foram identificadas fontes que podem causar poluição e discutidos os possíveis impactos no Parque Nacional Rio Formosa. Os resultados demonstram um aumento na intensidade dos eventos de inundação dos cenários T20 para os cenários T100, e também quando se propagam mais no futuro. Os valores mais

elevados relativos à profundidade e velocidade de inundação, perigo e risco de inundação concentram-se nas proximidades do rio Gilão (que atravessa Tavira) e diminuem à medida do afastamento deste curso de água. Grande parte da extensão da inundação afeta as salinas na parte sul da cidade.

Palavras-chave: análise de risco de inundação, avaliação de risco de inundação, alterações climáticas, curva profundidade-dano, mapas de risco

Table of Contents

List of Figures

List of Tables

1. Introduction

Natural hazards are defined as “unexpected and/or uncontrollable natural events of unusual magnitude that might threaten people” (Bokwa, 2013) that are linked to geophysical processes of the environment. There are different kinds of classification systems for natural hazards. The most common one is the classification according to the source or cause: geophysical (e.g., earthquakes, mass movements), hydrological (e.g., floods, landslides), climatological (e.g., droughts, wildfires), and meteorological (e.g., storms, extreme temperature) events or hazards. Other classification systems are, e.g., the time of the occurrence, the impact, or the predictability (Bokwa, 2013).

One of the most severe natural disasters regarding the occurrence, affected population, and economic damages are floods. In the time period from 1995-2015, they were responsible for 43 % of natural disasters worldwide according to the Centre for Research on the Epidemiology of Disaster and the UN Office for Disaster Risk Reduction. Natural disasters are compared to natural hazards, severe or extreme events where human lives and their belongings are affected (CRED & UNISDR, 2015). Floods, classified as hydrological events, go along with an enormous economic and social risk. In European Environment Agency (EEA) member states, they are responsible for 44% of the total economic losses resulting from natural hazards, followed by meteorological events (e.g., storms) with 34 %. Speaking in numbers, hydrological events caused 224 152 million € in damage over the period 1980-2020. The economic losses increased during the recent decades. That can mainly be explained due to a better reporting of floods and their losses and to socio-economic trends. Regarding fatalities, climatological sources (heatwave events) are clearly the “number one”. In the same time period, they caused 91% of total 142 101 fatalities. Floods follow on second position with “only” 4%. Besides human death, floods can impact human health in many other ways, such as heart attacks, injuries, infections, exposure to chemical hazards or mental health consequences. Besides that, the consequences of floods also include disruption of essential services (health services, water supply, infrastructure, etc.) (EEA 2017).

There are two main drivers that will increase the risk of flooding in the future: climate change and land use change. Because of the projected global warming, the hydrological cycle can be intensified in the future and thereby also the frequency and intensity of floods. In the past, the number of flood events increased already. For Portugal a decrease of 10-40 % in the annual precipitation by 2100 and on the other hand an increase in the frequency and intensity of heavy precipitation events is projected (Costa et al., 2012). Accompanied with heavy precipitation events are precipitation-generated floods (Hov et al., 2013). With the decrease in the annual precipitation, the risk of droughts increases. That is also important for the risk of floods because they are two hazards of the same hydrological cycle and therefore interact with each other, thus both hazards and potential risk reduction measurements can have positive and negative impacts on each other (Ward et al., 2020). For example, droughts can lead to increasingly hydrophobic soil properties and therefore to decreasing infiltration rates, hence, the impacts of extreme precipitation events can be intensified (Beisecker et al., 2020). Infiltration rates can not only be influenced by droughts but also by land use changes. Land use changes such as urbanisation, deforestation, or cultivation all lead to an increased flood risk trough, e.g., reduced infiltration capacity or lower soil porosity (Tollan, 2002). The process of urbanisation will go on in the future. It is expected that by 2050 the population in urban areas will reach 82 % of the total population (2011: 75 %) (UN HABITAT, 2011). Urban areas are more vulnerable to floods because of the agglomeration of people, their assets and economic activities (Guerreiro et al., 2018).

In order to assess and evaluate flood risk in the future and if necessary, take mitigation measures, the European Union passed a Directive on the assessment and management of flood risk with the overall

objective of reducing the negative impacts of flood on the health and safety of people and their property, on economic activities, infrastructure, cultural and historical heritage, and on the environment. The Directive requires all member states to establish flood hazard maps and flood risk maps. Flood hazard maps should cover different probability scenarios and should show the flood extent, the water depths of the floods and the flow velocity. Whereas flood risk maps should show the potential adverse consequences for the different probability scenarios expressed in terms of the indicative number of inhabitants, the type of economic activity, and installations concerning integrated pollution prevention and control that are potentially affected (EC, 2007). Portugal implemented this Directive through the Plano de Gestão de Risco de Inundações (PGRI) on a national scale in 2010. This plan defines measures to decrease adverse consequences emerging from floods in risk areas. The implementation was made in three phases and two planning cycles. Right now, the flood risk management plans from the first cycle for the time period from 2016 to 2021 are in force. Until now risk areas were selected and identified, then floods and exposed elements were mapped. Hence, the flood risk management plans were developed.

So far future flood scenarios were modelled for the river Gilão with information about the flood extent, the flood depth and the flood velocity. This was made within the flood risk management plans (PGRI) and published in the report "Security of People and Property- Current and Future Vulnerabilities" (Ferreira et al., 2019). To get the information the hydrological simulation model software MOHID Studio was used. The main objective of the master thesis is the creation of hazard maps (flood extent, flood depth, flood velocity), flood danger maps and the assessment of the economic, social, and environmental risk of floods in terms of two different return periods (T20 & T100) and three different future development scenarios (2011-2040, 2041-2070 & 2071-2100) and subsequently the creation of risk maps for each scenario.

2. Definitions

2.1 Floods

The European Union, in the framework of the EU Floods Directive, defines floods as "the temporary covering of land that is normally not covered by water". It includes floods with several different origins such as rivers, mountain torrents, Mediterranean ephemeral water courses or the sea in coastal areas. It does not include floods that emerged from a sewerage system (EC, 2007). Besides the different origins, floods area influenced by several factors such as precipitation, the relief of the river basin, soil and subsoil characteristics, the land use, and the regularisation of the watershed (e.g. dams or drainage systems) (Ferreira et al., 2019). But no matter what the origin or the cause for a flood is, all these distinct factors can lead to the same result: More water than the soil can capture or higher amounts of water than the artificial or natural run off capacity.

Floods are often described by means of their return periods. The return period refers to the average period of time between floods of a particular intensity. As an example, a return period of one hundred years does not mean that the flood occurs every 100 years, but rather refers to a flood that has a 1/100 or 1% chance of occurring in any one year. Return periods are based on historic conditions for a given area and are site-specific. They are not fixed, but can change with e.g. land-use change such as deforestation or urbanization, or climate change (Samuels & Gouldby, 2009).

2.2 Flood risk

Flood risk does not have one single definition in the common literature. The European Union defines it as "the combination of the probability of a flood event and of the potential adverse consequences for human health, the environment, cultural heritage and economic activity associated with a flood event" (EC, 2007). Schanze (2006) interprets flood risk "as harm to flood-prone elements with a specific vulnerability due to probable flood events". In a more mathematical way, flood risk can be expressed with the two following equations (Klijn, 2009):

$$risk = flood\ hazard * exposure * vulnerability \tag{2.1}$$

$$risk = probability\ of\ the\ flood * consequences \tag{2.2}$$

The term flood hazard, which is part of the first equation, is defined as "the probability of the occurrence of potentially damaging flood events" (Schanze, 2006). The flood hazard considers flood events with different features. For example, one single house can be affected by a flood with a return period of one hundred years, but not with a return period of 20 years. Simply put, flood hazard just shows areas or elements that might be affected by a flood (Schanze, 2006). The term 'exposure' only means if the element is effected by a certain flood depth and is either 0 (not exposed) or 1 (exposed) (Klijn, 2009). Vulnerability defines the resilience of an element such as houses or human beings when exposed to a flood (Dias et al., 2014).

Using the term risk, the probability or likelihood of a flood occurring plays a key role in order to evaluate the importance or necessity of risk mitigation or adaptation. Simply put, when the probability of a flood event is really high, risk adaptation is more necessary, than for floods with a smaller probability. This problem is better addressed in the equation 2. Here, the specific probability of a flood is necessary, as well as the negative adverse consequences in order to calculate the risk. Negative consequences, for example, can be expressed in economic (monetary) damage, the impacts on the society or the environment (EC, 2007).

Another way to describe the term flood risk is the conceptual Source-Pathway-Receptor-Consequence-Model (SPRC-Model) (Figure 2.1). It illustrates the flood risk as a logical causal chain starting at the source (meteorological or hydrological events), over the surplus water way (pathway) until it reaches the elements at risk (receptor) such as property, people, or environment. As a last link the consequences that might occur are presented, such as death, stress, material damage, or environmental degradation. The previously mentioned terms of flood hazard and vulnerability are also kept in mind in this description (Schanze, 2006).

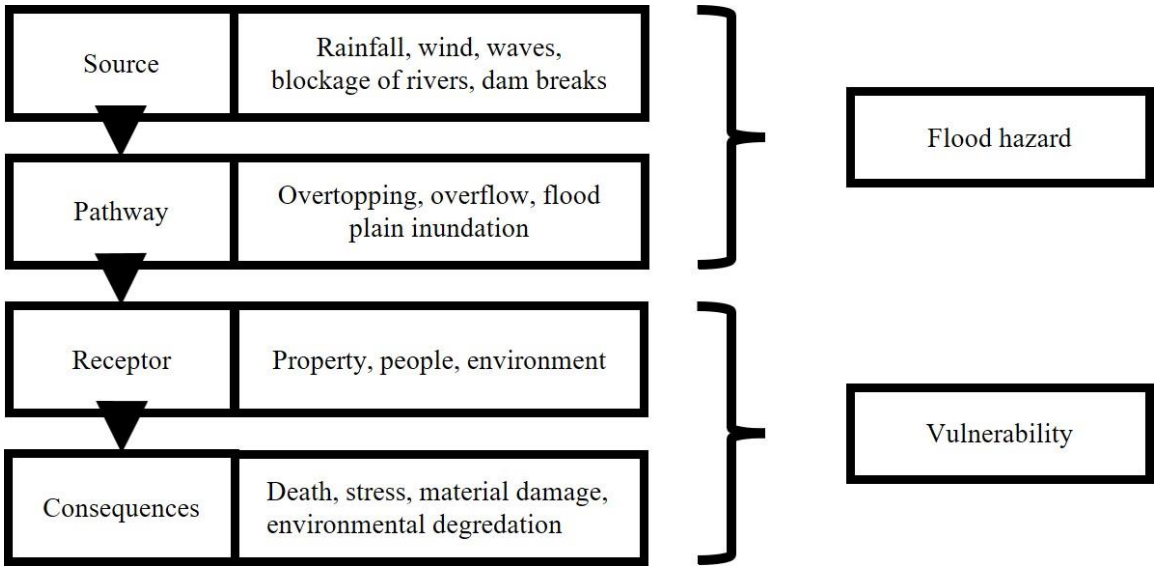

Figure 2.1: Source-Pathway-Receptor-Consequences-Model for flood risk showing the way from the water from its source until the consequences. Adapted and modified from Schanze (2006).

2.3 Flood risk management

Since changes in precipitation and temperature are likely to occur in the near future (Pachauri et al., 2014) and this will be accompanied by floods, it is important to develop strategies to adapt to those changes. Flood risk management plans are based on available information such as records and studies (models) on the long-term development of the occurrence of floods. Therefore, areas that have a significant flood risk or where they are likely to occur have to be determined (EC, 2007). To accomplish a risk management plan, three different steps have to be conducted: a risk analysis, a risk assessment and a risk mitigation. The risk analysis includes the determination of the hazard, the vulnerability, and the risk itself. The scientific analysis of these factors, results in an assessment of the risk. The approach of classifying the hazard, vulnerability, and risk depends on individual and collective perceptions by the society as well as the tolerability of the risk. Simply put, the overall question in risk assessment is: How much risk is tolerable considering the expected costs and benefits? The last part of the risk management plan is the risk mitigation: If areas with a not tolerable risk are identified, measures and instruments have to be applied for a reduction of the risk. That means not only the reduction of potential damage, but also the reduction of a flood event happening in the first place. Here again a simple question can be asked to the people in charge: Where is the risk unacceptably high and where are mitigation actions necessary (Schanze, 2006)? This master thesis will focus on risk assessment using available data on risk analysis.

2.4 Depth-damage curve

A useful tool of risk assessment are depth-damage curves or vulnerability curves. They show the graphical relationship between the water depth caused by a flood and the expected monetary damage. Figure 2.2 shows an exemplary depth-damage curve for residential buildings in mainland Portugal. On the x-axes the water depth in m and on the y-axes the monetary damage in Euro per m^2 is presented.

Most of the time, depth-damage curves present different curves for different elements at risk, such as residential or commercial buildings. Depth-damage curves are often used to determine the economic damage caused by a flood, but it is important to mention, that the caused damage does not only depend on the water depth. Other factors such as the flood duration, the time of the year the flood occurs, the water velocity, and suspended debris also have an impact on the damage. To obtain a higher certainty of the potential damage, it is therefore important to find a suitable depth-damage curve for the study area (Martínez-Gomariz et al., 2020a).

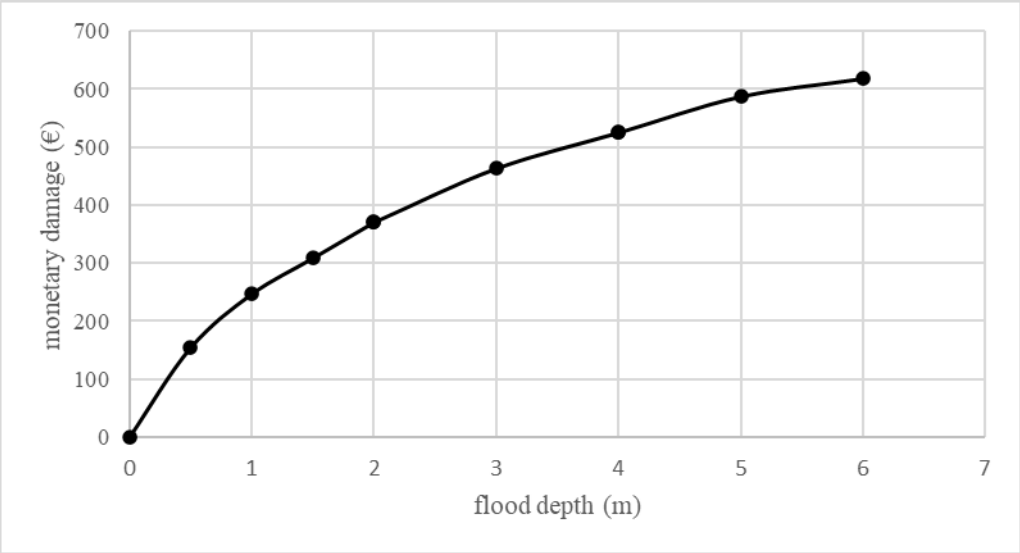

Figure 2.2: Exemplary depth-damage curve for residential buildings in the study area with information from Huizinga et al. (2017).

2.5 Damage-probability curve

To assess the last step of the flood risk analysis (the actual risk) damage-probability curves can be applied in order to conclude the risk assessment. Damage-probability curves show the probability on the x-axis and the damage on the y-axis. An example of a damage-probability curve is shown in Figure 2.3. By constructing such a curve, the actual expected damage can be presented graphically. Hereby, the probability is equivalent to the different observed return periods and the damage with the calculated damage for this return period. Analogous to the depth-damage curve, different curves can be constructed for the different land cover classes (e.g., commercial, residential, etc) or summarized in just one curve with the total damage for the study area. The expected annual damage is calculated as the integral and is equal to the risk.

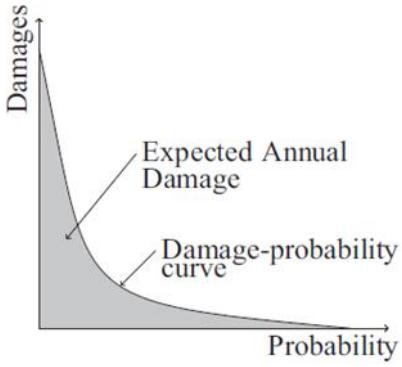

Figure 2.3: Exemplary Damage-Probability curve (Foudi et al., 2015).

3. Study area

The city of Tavira is located in the southeast of Portugal (Figure 3.4) in the Tavira municipality (Faro District) and has around 15000 inhabitants. The Gilão River is traversing right through the middle of the town, which makes the city susceptible to river floods. (Foudi et al., 2015)

According to the Köppen-Geiger classification the region belongs to the 'warm temperate with dry, hot summer' (Csa) class, which is characterized by winter mild months, that are warmer than -3°C but colder than +18°C, whereas the summers are dry and hot (Kottek et al., 2006).

The catchment area of the Gilão river which has an area of 237 km^2 is shown in Figure 3.4. The source of the River Gilão is located in the Serra do Caldeirão mountains in the Algarve. In the upper parts the river is called Séqua. It changes its name in the middle of Tavira city to Gilão.

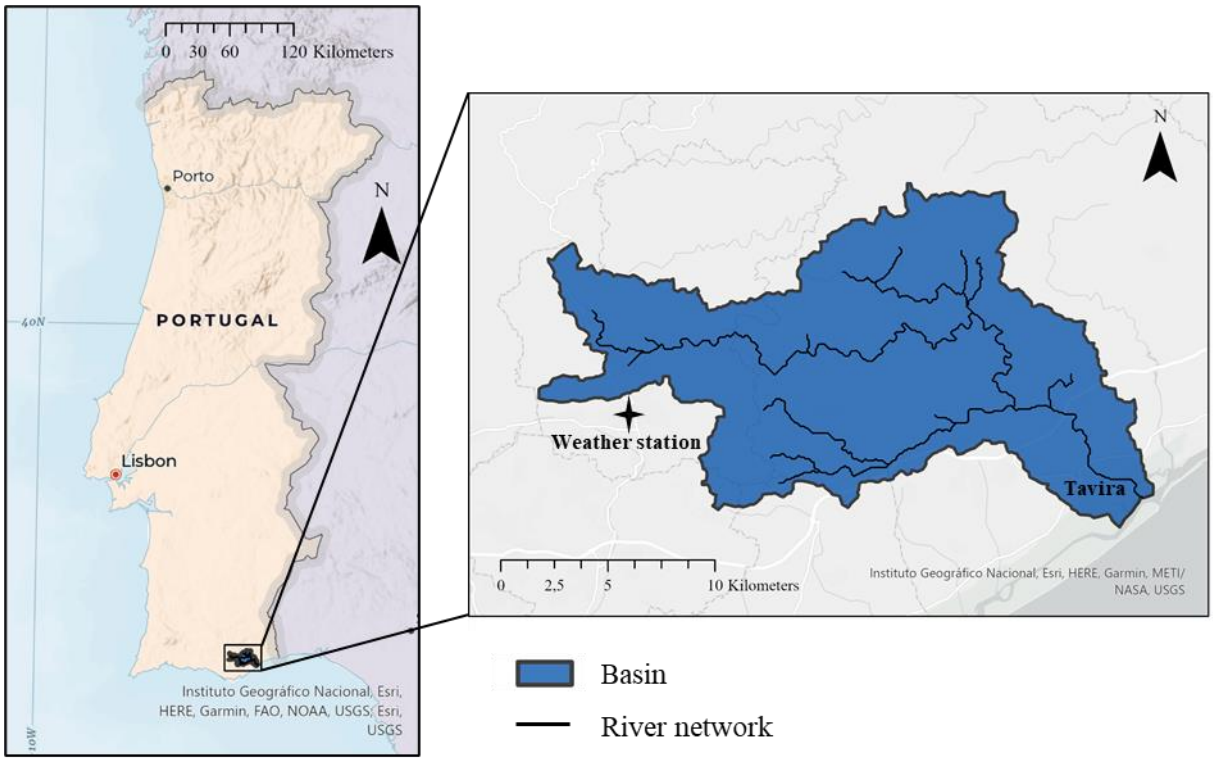

Figure 3.4: Basin area of the river Sequa and river Gilão with the weather station in São Brás de Alportel.

The city of Tavira has a long history, the presence of human life in this area reaches back to the Neolithic period (4.000 to 1.500 B.C.). Therefore, there are a lot of historic buildings such as churches or the remaining parts of the castle and its wall. That historical heritage increases the vulnerability to floods for the area (Região de Turismo do Algarve, 2013). Besides those old sensitive buildings, other buildings, or infrastructure such as the Municipal Council, the Parish Council, gas stations, railroad of the Algarve Line, etc. can be found in the floodplain area. Also, at the southern part of the basin natural heritage and protected areas can be found. These include RAMSAR (Convention of Wetlands), SIC (Sites of Community Importance), SPA (Special Protection Areas) and RNAP (National Network of Protected Areas) sites (Guadiana, 2020). All of them are located in the National Park of Ria Formosa, which was declared with this designation in 1987 and has an area of about 18000 hectares and a length of around 55 km along the east Algarve. It is particularly known for many bird species coming from northern Europe on their way to the south (Bebianno, 1995).

Figure 3.5 shows the Digital Elevation Model on the left side and the slope on the right side. The elevation ranges from 0 to 514 m in the basin. The decrease in elevation from the northern part of the basin to the southern part can be clearly seen in the slope map. The city of Tavira is located in the southern part of the basin with a lower elevation, which leads to an accumulation of water coming from the higher parts. This is also promoted through the high slopes in the northern part with a decrease towards the city of Tavira. Because of the steepness, some areas are almost vertical, in the northern part, in case of a heavy rain event, the surface discharge can be extremely fast and high.

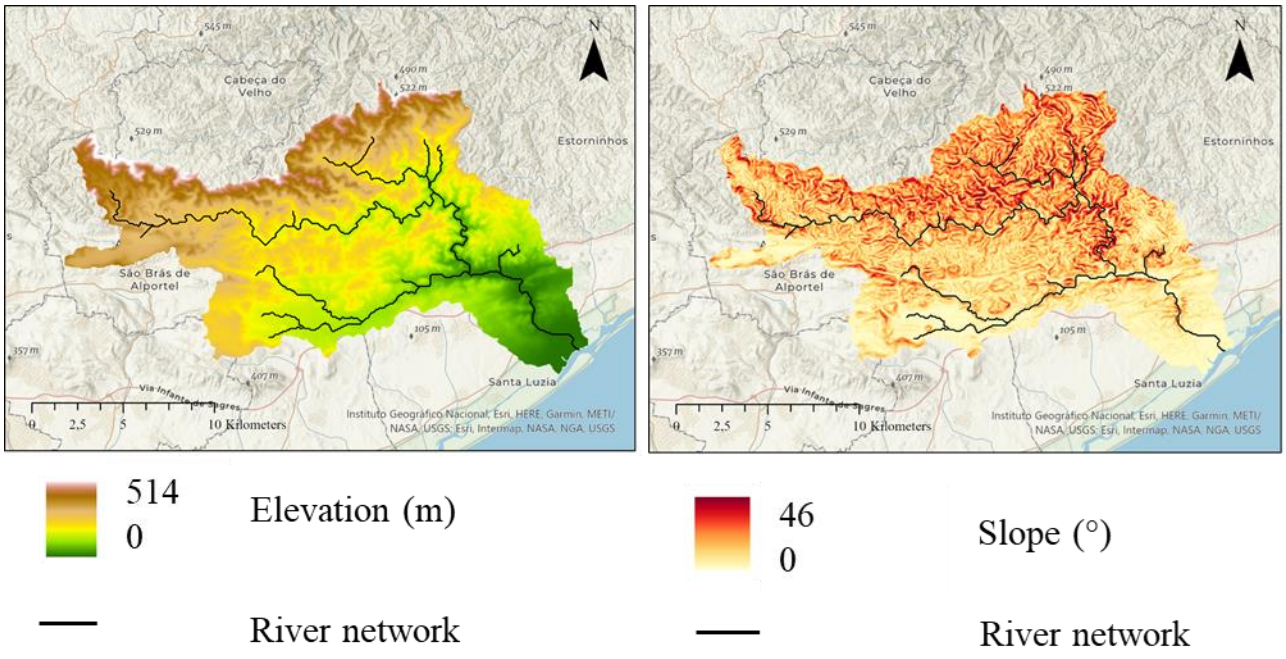

Figure 3.5: Digital Elevation Model (left) and Slope map (right) of the basin area for river Gilão.

In total three main criteria can be named to justify why this area was selected as a study area:

1. Vulnerability of the area
2. Susceptibility of the area
3. Availability of data

The data is provided by the Sector report "Security of People and Property- Current and Future Vulnerabilities", which is part of the Climate Change Adaptation Plan for the Algarve region (Ferreira et al., 2019). The report obtains information about the flood extent, the flood depth, and the flood velocity for the return periods T20 and T100 for three developments (short, mid, and long term), that were calculated based on the following two steps:

1. Compilation of the necessary information (topographical data, thematic cartography, hydrology, meteorology)
2. Hydrological and hydraulic modelling

The hydrographic basin in which Tavira is located, does not have any flow regulations (e.g., dams) which simplifies the hydrological modelling. To determine the flood tip flow rates the MOHID Studio software was used (Ferreira et al., 2019).

The flood risk management plan also identifies the Tavira area as vulnerable due to river or estuarine floods (APA, 2015). Therefore, it is important to get a better knowledge about potential features of future floods. One criterion of why this area was chosen refers mainly to the land cover of Tavira. Since it is an urban area, it is more susceptible to floods because of two main criteria: the natural water cycle is interrupted because of the sealed areas and therefore more water is available for flooding and on the other hand the economic damage is much higher than in rural areas.

Besides that, climate change will alter the precipitation in the near future, which makes a risk assessment even more necessary. Table 3.1 shows precipitation data for São Brás de Aportel in mm for the two return periods T20 and T100. The location of the weather station, which precipitation data was used for the flood modelling, can be seen in Figure 3.4. The first column presents historical data, and the following columns present data that was calculated and modelled for the previously mentioned sector report (Ferreira et al., 2019). As it can be observed, the precipitation values are increasing in every climate change scenario. The lowest value is for the return period of 20 years for the historical data (117.9 mm). It increases for every development and every climate change scenario until the highest value for the time period 2071-2100 and the climate change scenario RCP8.5 (170.1 mm), which would be an increase of 44%. For T100 the precipitation values range from 147.8 mm (historical data) to 245.9 mm (time period 2071-2100, RCP8.5), which would be an increase of 66%.

Table 3.1: Precipitation data in mm for the study area (Ferreira et al., 2019).

	1955-2002	**2011-2040**		**2041-2070**		**2071-2100**	
	historical	RCP4.5	RCP8.5	RCP4.5	RCP8.5	RCP4.5	RCP8.5
T20 (mm)	117.9	158.0	138.5	164.9	147.9	154.4	170.1
T100 (mm)	147.8	206.7	178.1	215.4	190.3	200.4	245.9

All these mentioned factors from the historic and natural heritage, the increased hazard due to climate change, land use change to the risk depending on the predominant climate in that region, contribute to a possible high flood risk, which makes it important to assess future floods events.

In general, the basin area for the Gilão river can be interpreted as the study area because it is important to understand why the city of Tavira is endangered by floods and the source of possible floods is located there. But yet the risk assessment takes place on a smaller scale because the flooding occurs not at the macro but the microscale; particularly at the location of the city of Tavira (Figure 3.6).

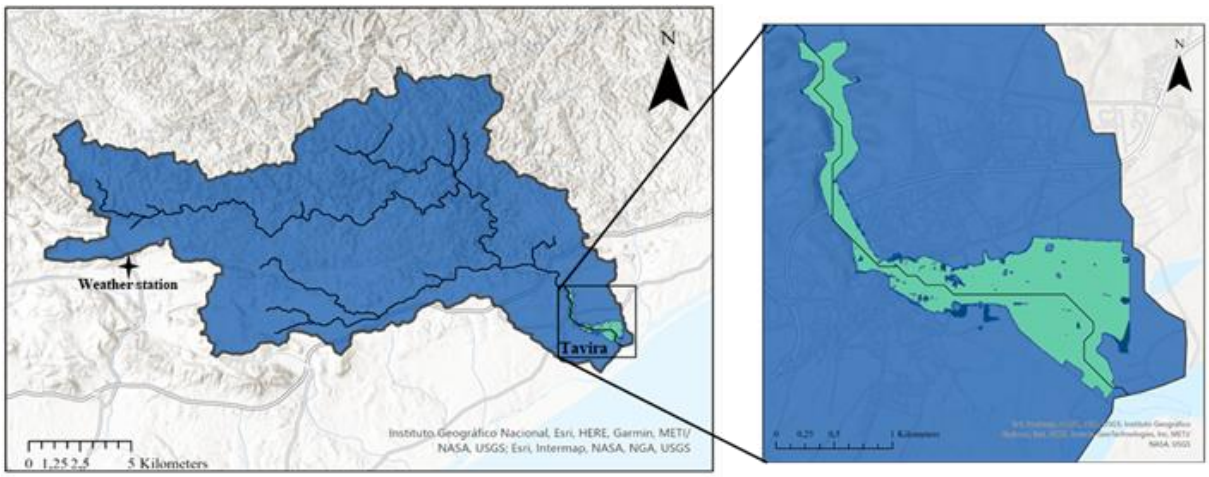

Figure 3.6: Location of the risk assessment maps in the whole basin.

4. Methodology

To comply with the EU-Directive different kinds of maps have to be determined in order to assess and analyse the risk (risk analysis and assessment).

The necessary flood data (flood extent, flood depth, and flood velocity) to construct the flood hazard maps, the flood danger map, and the flood risk maps were provided by the "Security of People and Property- Current and Future Vulnerabilities" (Ferreira et al., 2019) report. The report provides information for two historical flood events and six future scenarios. Table 4.2 shows the historical precipitation data and the calculated precipitation for the future scenarios given from Ferreira et al. (2019). The precipitation was calculated for the Representative Concentration Pathways (RCP) 4.5 and 8.5. The precipitation data represents the basis for the model calculations to obtain the flood data. The RCP scenarios with the highest precipitation levels in their respective timeframes are framed in red. To calculate the flood extent, the water depth, and the water velocity, the study used the hydrological simulation model software MOHID Studio. The model is based on topographic and hydrological data.

Table 4.2: Precipitation data in mm for the study area with the used highest precipitation value for each return period and development marked in red (Ferreira et al., 2019)

	1955-2002	**2011-2040**		**2041-2070**		**2071-2100**	
	historical	RCP4.5	RCP8.5	RCP4.5	RCP8.5	RCP4.5	RCP8.5
T20 (mm)	117.9	158.0	138.5	164.9	147.9	154.4	170.1
T100 (mm)	147.8	206.7	178.1	215.4	190.3	200.4	245.9

In total there are two flood events from the historical data (1955-2002) for the two return periods (T20, T100) and two future scenarios for each temporal development (short term (2011-2040), mid term (2041-2070), long term (2071-2100)) for the two return periods (T20, T100):

1. T20-historical
2. T100-historical
3. T20-short term
4. T100-short term
5. T20-mid term
6. T100-mid term
7. T20-long term
8. T100-long term

The information from the sector report was given as a layer with simple polygon feature classes, which can be processed in ArcGIS Pro. The layers consist of several small polygons with a size of 4,44 m x 5,55 m (24.642 m^2). The quantity of those polygons depends on the scenario and particular size of the flood extent. The polygons contain information about the flood depth and the flood velocity at their location. The spatial reference of the maps is the ETRS 1989 Portugal TM06 coordinate system. An extract of the attribute table for one of the scenarios (T100-longterm) can be seen in Figure 4.7. The column 'MaxWC' refers to the water depth and the column 'VelMaxWC' to the water velocity. These two columns were further processed to create the flood hazard and flood risk maps as described in the next section.

	FID *	Shape *	I	J	MaxWC	MaxWL	VelMaxWC	MaxHazard	Shape_Length	Shape_Area
1	1	Polygon ZM	1	316	0,047	2,0474	0,161	0,0311	19,986063	24,65974
2	2	Polygon ZM	1	317	0,0468	2,0507	0,0939	0,0278	19,986164	24,660075
3	3	Polygon ZM	1	318	0,0443	2,0522	0,0605	0,0248	19,986164	24,660075
4	4	Polygon ZM	1	319	0,0421	2,0528	0,0403	0,0228	19,985964	24,65952
5	5	Polygon ZM	1	320	0,0416	2,0531	0,0252	0,0219	19,986164	24,660075
6	6	Polygon ZM	1	327	0,0437	2,0499	0,1069	0,0265	19,986064	24,659798
7	7	Polygon ZM	1	328	0,0435	2,0452	0,1873	0,0299	19,986164	24,660075
8	8	Polygon ZM	1	329	0,0327	2,0297	0,306	0,0263	19,986165	24,660022

Figure 4.7: Exemplary attribute table for the scenario: T100 long term (2071-2100).

4.1 Construction of the flood hazard maps

4.1.1 Flood extent map

The flood extent maps were created using the geoprocessing tool 'Dissolve' in order to get one big polygon that covers all the small polygons in the layer file. Figure 4.8 shows the modelbuilder workflow used for the construction. The newly created polygon covers the whole area of the flood extent and was obtained from the new attribute table.

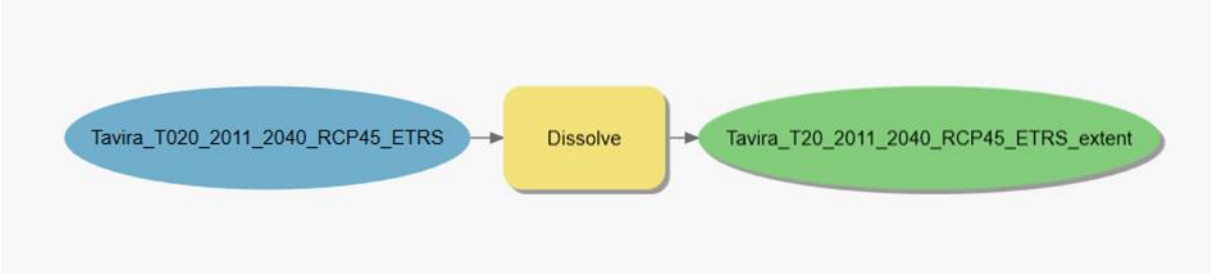

Figure 4.8: Modelbuilder workflow for the construction of the flood extent maps.

4.1.2 Flood depth maps

To create the flood depth maps, the input data was converted to a raster file using the height of the water column (see column 'MaxWC' from Figure 4.7). This was done using the geoprocessing tool 'Polygon to Raster' (Figure 4.9). The cell size for the built raster is 0.05 m, which is an area of $2.5*10^{-3}$ m^2. This cell size provides a sufficiently detailed map for further calculations (displaying the extent of buildings).

Figure 4.9: Modelbuilder workflow for the construction of the flood depth maps.

4.1.3 Flood velocity maps

The same process was used to create the velocity maps of the scenarios. But instead of the water depth (column 'MaxWC'), the water velocity (column 'VelMaxWC') was used to build the raster. The cell size is again 0.05m.

4.2 Construction of the flood danger maps

Flood danger maps combine different flood parameters in order to obtain a degree of danger. Guadiana (2020) proposes the danger (D) as a function of the height (h in m) and the velocity (v in m/s):

$$D = h \times (v + 0.5) \tag{4.1}$$

This approach was used to create the flood danger maps for the study area. The calculated danger can then be assigned to a danger class:

Table 4.3: Danger classification ranging from non-existent to very high (Guadiana, 2020).

Danger (D)	Class
<0.75	1- non-existent
0.75-1.25	2- low
1.25-2.5	3- average
2.5-7	4- high
>7	5- very high

To calculate the danger in ArcGIS the geoprocessing tool 'Calculate Field', which calculates a new column in the attribute table, was used. For the depth the column 'MaxWC' and for the velocity the column 'VelMaxWC' was inserted. Afterwards, the same procedure to construct a raster (here based on the danger values), as before for the other hazard maps, was used. Based on the new calculated field, the raster was constructed and classified according to the danger classes (Table 4.3, Figure 4.10). Therefore, the geoprocessing tool 'Reclassify' was used, which assigns the danger classes (1-5) to the calculated danger (D).

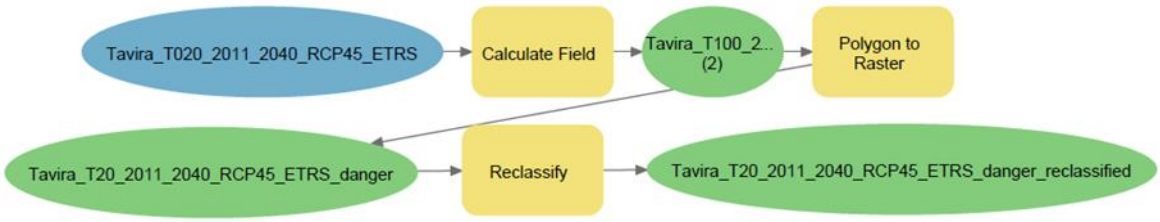

Figure 4.10: Modelbuilder workflow for the constructing of the flood danger maps.

4.3 Calculation of the economic risk

The previously created flood depth maps are one part in calculating the economic damage. The annual average damage (=economic risk) can be calculated through the absolute economic damage per event. The methodology to obtain the economic risk for the three different time periods (developments) can be divided into different steps:

1. Survey of the land cover
2. Preparation of depth-damage curves

3. Connection of the landcover, the economic damage, and the water depth
4. Calculation of the absolute economic damage per event
5. Preparation of the probability damage curves
6. Calculation of the economic risk

The steps were conducted with ArcGIS Pro and Microsoft Excel.

4.3.1 Survey of the land cover

The information of the landcover was obtained from two independent sources: Municipality of Tavira and Google Maps. The Municipality of Tavira offered KML-files with information about the location of buildings and their content, and the road network. The KML-files were converted to feature classes (polygons) and layer files with the geoprocessing tool 'KML To Layer'. The information was verified with Google Maps and complemented in case of missing or incorrect information. The landcover had to be divided into different classes according to the depth-damage curves. The depth-damage functions proposed by the European Union (Huizinga et al., 2017) have six different classes: Residential, Commerce, Industry, Transport, Infrastructure, and Agriculture. The information about the infrastructure was just the road net as a Line feature class. To create an area with the full road extent, the geoprocessing tool 'Buffer' with a distance of 3 m was used. So in total a road width of 6 m was created. Martínez-Gomariz et al. (2020) proposed different depth-damage curves for several Spanish cities. For this thesis, the depth-damage curve from Los Alcázares (Spain) was used. It was selected because the city has a similar population and latitude as the study area. This type of curve does not exist for Tavira or a similar city in Portugal. Here, the depth-damage curve is divided into more specific classes: Warehouses, Car park, Restaurant, General trading, Homeowner association, Sport, Education, Hotel, Industries, Office, Health, Workshop, Dwelling, Churches and Singular buildings. According to the respective curve, the landcover was divided into these classes. For the Spanish depth-damage curve the commerce class from the EU was further divided into Warehouses, Restaurants, General trading, Sport, Education, Hotel, Office, Health, Workshops and Churches. The other classes (Industries and Dwelling) were not used from the Spanish curve, because they are the same classes as for the EU depth-damage curve, just with more inaccurate damage values, because the values were obtained based on the Spanish economy and not the Portuguese one.

4.3.2 Preparation of depth-damage curves

Huizinga et al. (2017) provides fractional depth-damage functions and the maximum damage that occurs at a water depth of six meter for each country and for each class (Residential, Commerce, Industry, Transport, Infrastructure, and Agriculture). Exemplary, Figure 4.11 shows the flood depth in meters and the associated fraction of the maximum damage. From the given maximum damage, the associated damages in € per m^2 can be calculated by using the following equation:

$$Damage = fraction\ amount \times maximum\ damage \quad (4.2)$$

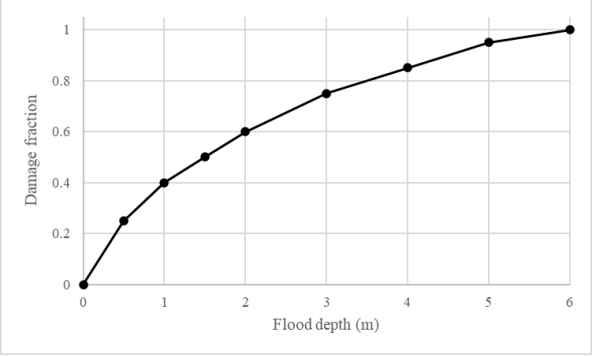

Figure 4.11: Depth-damage function for residential buildings in Portugal (Huizinga et al., 2017).

For each of the above mentioned class the respective damage caused by different water depths, can be calculated.

By using equation (4.2) and the data from Huizinga et al. (2017) for Portugal the depth-damage curves for the six landcover classes were created (Figure 4.12). The landcover classes Agriculture and Infrastructure have, compared to the other classes, the lowest economic damage (in €/m²). The underlying fractional functions for the landcover classes are in Appendix A.

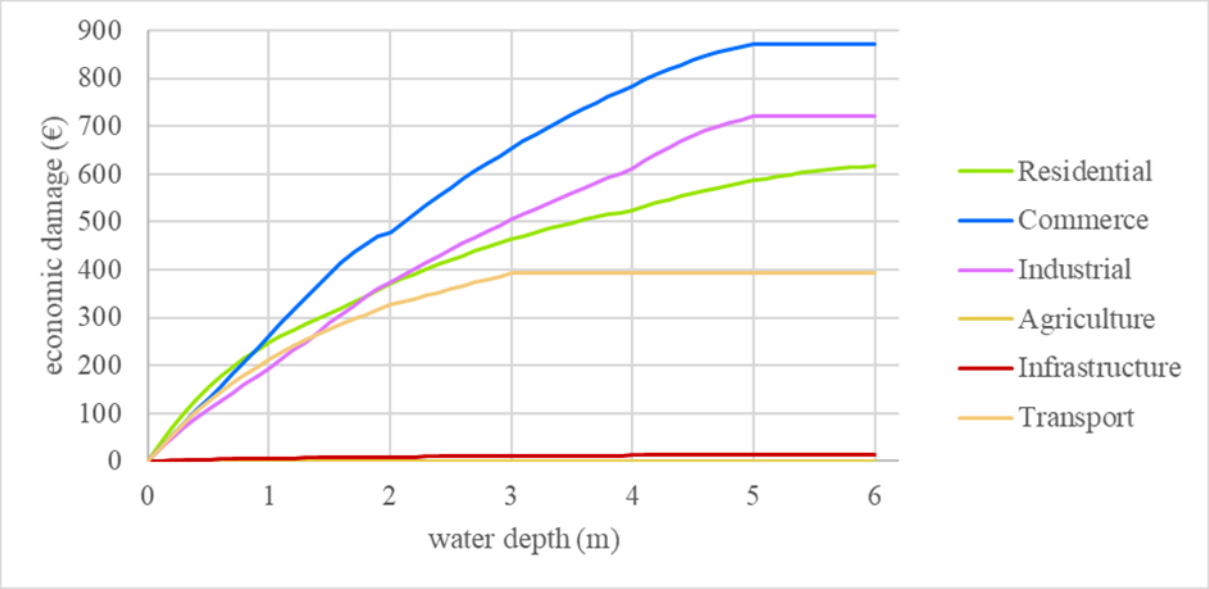

Figure 4.12: Depth-damage curve for the six landcover classes Residential, Commerce, Industrial, Agriculture, Infrastructure, and Transport.

The data from the depth-damage curves from Los Alcázares was modified in order to get a better fit for Portugal. For the adjustment, the maximum damages from Spain and Portugal were compared (both known from Huizinga et al. (2017)). According to the proportional difference the damages for Los Alcázares were adjusted. Figure 4.13 shows the more segmented depth-damage curves for the commerce landcover class based on the data from the Spanish city Los Alcázares (Martínez-Gomariz et al., 2020). It was divided into Restaurant, General trading, Sport, Education, Hotel, Office, Health, Workshop, Churches and Singular buildings. For a better comparison, the landcover class commerce is also shown. The sub-class health has by far the highest economic damage (in €/m²). Compared to the commerce landcover class it is almost twice the damage. The other sub-classes show less economic damage. Besides the health sub-class, most of the other sub-classes show similar damages until a water depth of 0.5 m and then the commerce curve increases faster than the other sub-classes. At a water-depth of 3 m Restaurants (compared to the other sub-classes besides from Health) show the highest damage, followed by General trading, Office, Education and so on.

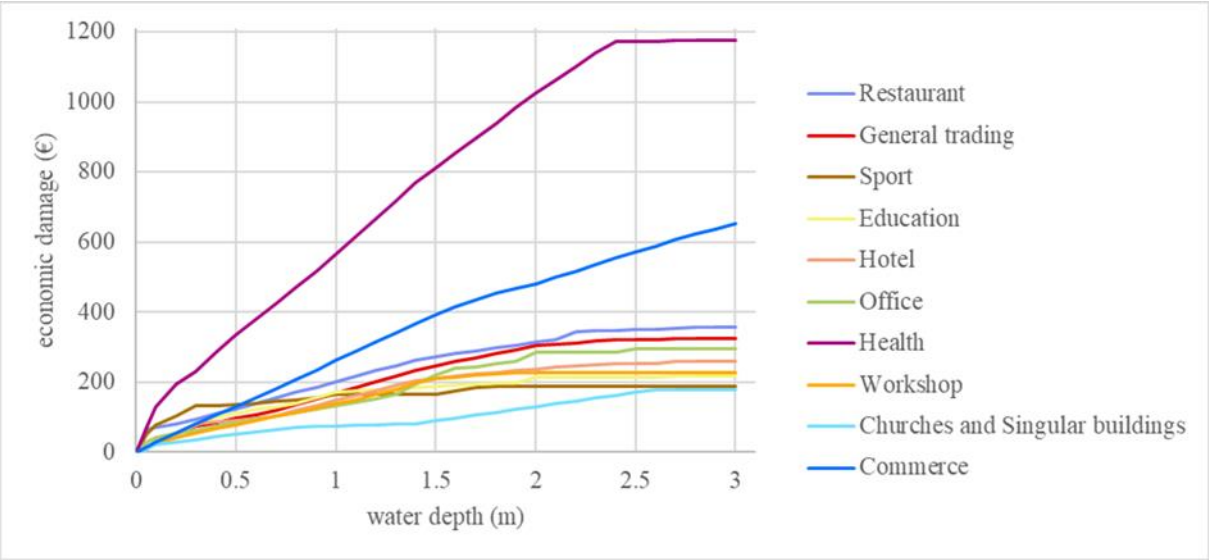

Figure 4.13: Depth-damage curve for the nine landcover classes Restaurant, General trading, Sport, Education, Hotel, Office, Health, Workshop, Churches and Singular buildings. For a better comparison, the landcover class Commerce is also shown.

4.3.3 Calculating the absolute economic damage

The following workflow to calculate the economic damage was performed for each scenario. To determine the economic damage for each land cover class and water depth, the landcover information and the damage per depth have to be connected. As input data, the already created depth raster (see 4.1.2 Flood depth maps), where every cell corresponds to the associated depth, was used. The cell size was set to 0.05 m, in order to display the shape of the buildings as exact as possible.

As a next step, the depth information per cell was converted to the monetary damage with the geoprocessing tool 'Reclassify'. Figure 4.14 shows an extract of the conversion table for residential buildings. Each water depth corresponds to a monetary value depending on the landcover class (e.g., Residential). The first two column 'Start' and 'End' refer to the water depth in 10 cm steps and the third column 'New' is the corresponding monetary damage in €/m^2. This information was calculated previously with the depth-damage curves. After that, the absolute monetary damage per raster or event was calculated, using the ArcGIS Statistics tool.

Start	End	New
0	0,1	0
0,1	0,2	37
0,2	0,3	71
0,3	0,4	102
0,4	0,5	129
0,5	0,6	154
0,6	0,7	177
0,7	0,8	197
0,8	0,9	215
0,9	1	232
1	1,1	247
1,1	1,2	261

Figure 4.14: Extract of an exemplary table for the conversion from the depth to the damage.

4.3.4 Preparation of the probability-damage curve

In order to calculate the economic risk or the average annual damage, probability-damage curves were generated to illustrate the risk. They show the expected damage of a flooding event combined with the probability of occurrence. Ideally, they are created with as many flood scenarios as possible in order to obtain the best estimates of the risk. Since, in this thesis only the data for two scenarios (T20=0.05 and T100=0.01) were available, the probability-damage curves do not reflect the actual risk with precise enough accuracy. Therefore, the calculations were simplified. On the y-axis of the probability-damage curve the calculated damage is shown with the corresponding probabilities on the x-axis. The generation of the curve was done for every development: short, mid, and long term. Theoretically, for each raster cell depending on its calculated monetary damage, one single probability-damage curve can be created. But since probability-damage curves are more helpful in understanding what the risk is, and not necessary to calculate the actual risk, that was not done. The total damage is the integral of the probability-damage curve.

4.3.5 Calculating the economic risk

To calculate the risk (or annual average damage), the integral of the probability-damage curve was calculated. To calculate that area the following steps were applied.

First, the mean damage of two known points (damage for the two respective return period or probability (P)) of the curve (D[i]) was calculated using the following equation (DVWK, 1985):

$$D[i] = \frac{D(P_{i-1}) + D(P_i)}{2} \tag{4.3}$$

Since only two points of the probability-damage curve are known the mean damage had only been calculated once. This was done using the geoprocessing tool 'Plus' in ArcGIS. As input raster the previously calculated raster for the probabilities T20 (=0.05) and T100 (=0.01) that show the monetary damage per m^2 were used. With the square area of 0.0025 m^2 per raster cell and the area specific damage (D_{m^2}) the total monetary damage per raster cell can be computed:

$$D_{cell} = D_{m^2} \times 0.0025 \tag{4.4}$$

Now equation (4.3) was applied in ArcGIS using the geoprocessing tool 'Calculate Field'. Since the numerator of the equation was already calculated before using the geoprocessing tool 'Plus', the monetary damage had only been divided by 2.

The annual average damage can be calculated by using the following equation (DVWK, 1985):

$$\overline{D} = \sum_{i=1}^{k} D(i) \times \Delta P_i \tag{4.5}$$

Where ΔP_i was calculated by using the following equation:

$$\Delta P_i = |P_i - P_{i-1}| \tag{4.6}$$

Since there were only two known points of the damage-probability curve, this calculation had only been applied once with P_i=0.01 (T100) and P_{i-1}=0.05 (T20).

As a result, the annual average damage (=economic risk) per cell was calculated. In order to show the calculated risk results in the raster, the geoprocessing tool 'Lookup' was used.

The obtained values were divided into 10 classes reaching from 0 (no risk) to 10 (highest risk).

Figure 4.15 shows the complete workflow that was used for calculating the economic risk.

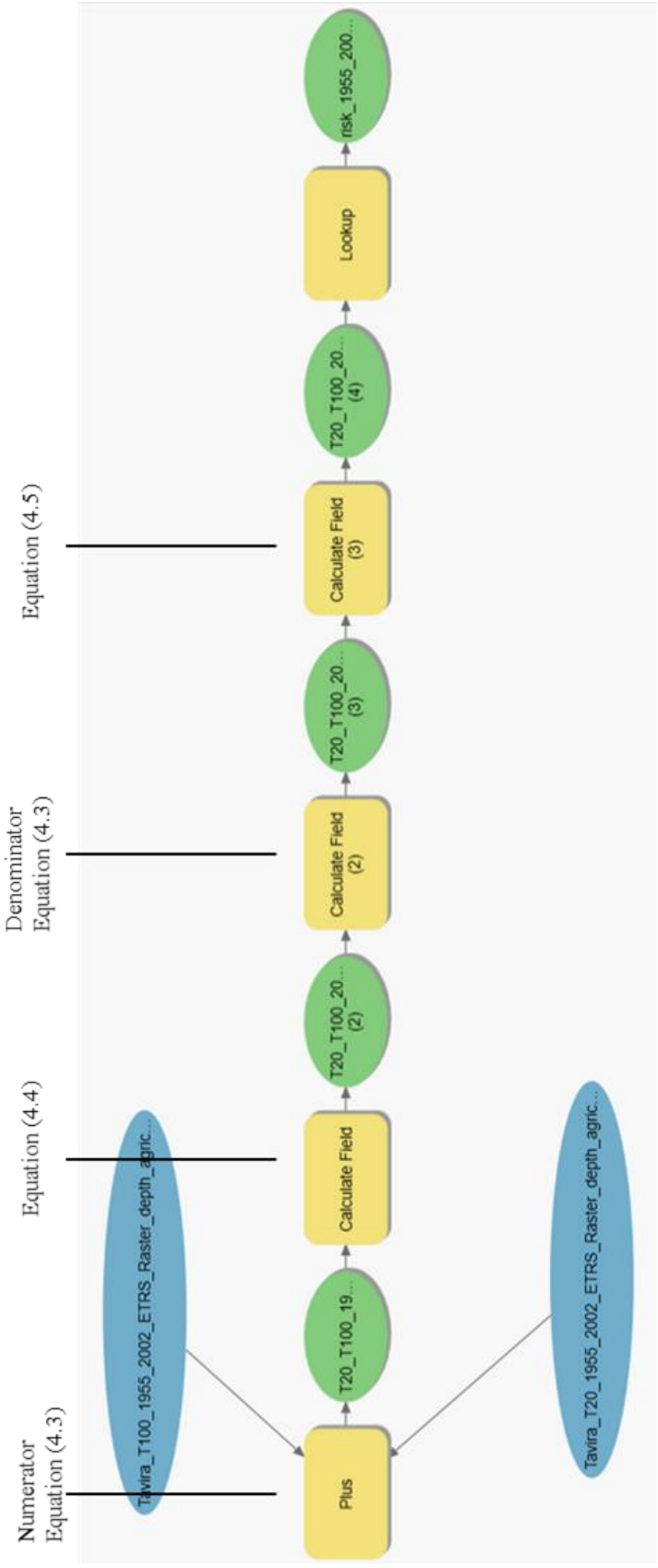

Figure 4.15: Modelbuilder workflow for calculating the economic risk.

4.4 Determination of the social risk

Besides the economic risk, the social risk can be determined. Meyer et al. (2009) states that social effects of flooding are often not considered because they are not as easily measured as the economic damage. Therefore, the paper proposed to evaluate the social risk in terms of the annual average affected population and the probability of vulnerable community locations of being affected. The measurement unit hereby is not in Euro but in number of people affected, and affected yes or no, respectively. Through this process the impacts on the society can be measured, too.

The social risk includes two criteria: probability of social hotspots such as hospitals, schools, or residential home for the elderly being affected, and the annual affected population.

4.4.1 Probability of social hotspots being affected

For the first criterion, the already gathered information about the landcover classes were used and social hotspots identified. To simplify the process, it was assumed that each of the sensitive building has the same vulnerability, regardless of the size of the building or other factors. By using the geoprocessing tool 'Clip', the relevant buildings for each scenario were extracted (Figure 4.16). To determine the buildings per development (short, mid, and long term) that are affected by both return periods, the geoprocessing tool 'Count Overlapping Features' was applied (Figure 4.17). As a result, it provides one file per development with the information 1 (affected by the T100 scenarios) or 2 (affected by the T20 and T100 scenarios).

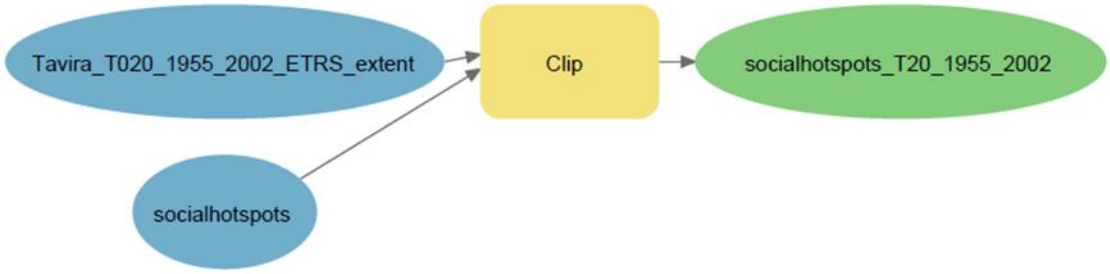

Figure 4.16: Modelbuilder workflow for extracting the relevant buildings for each scenario.

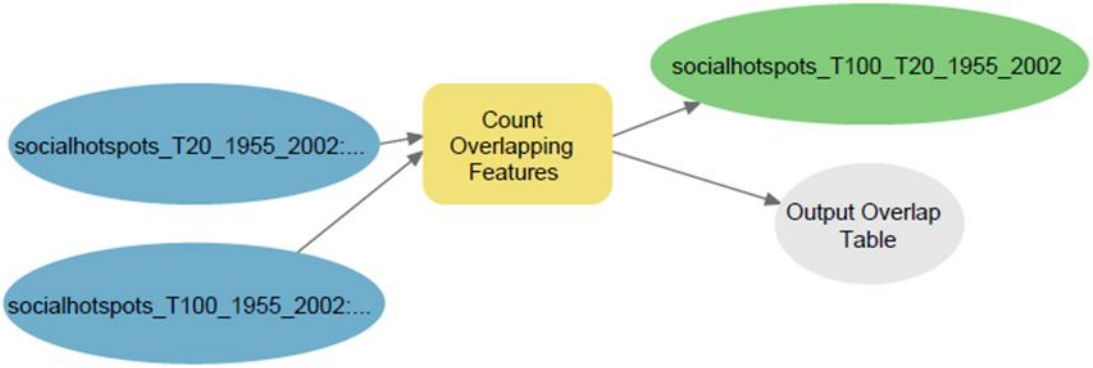

Figure 4.17: Modelbuilder workflow to identify the buildings, that are affected by both return periods.

4.4.2 Annual average affected population

For calculating the annual affected population, first the absolute number of affected people per scenario was calculated. Therefore, the extent of the flooded area (in m^2), determined by using the Statistics tool, and the previously created maps of the flood extent were used in the following expression:

$$total\ amount\ of\ affected\ inhabitants = flooded\ area \times population\ density \qquad (4.7)$$

To determine the average affected population, the same workflow as for calculating the economic damage was performed (applying equation (4.5)). However, instead of the monetary damage, the amount of affected people per area was used.

4.5 Determination of the environmental risk

The same problem as for the social risk, arises from assessing the environmental risk. There are different approaches to evaluate the environmental risk, e.g., determination of the erosion and accumulation potential (Meyer et al., 2009). Because there is no easy way to measure the risk for the environment in monetary units, the European Commission proposes to include "[..]information on potential sources of environmental pollution [..]"(EC, 2007). Therefore, sources that might cause pollution have been identified. Buildings in the potential flooded area that might cause pollution such as pumping stations were identified and the probability of them being affected was calculated the same way as the social hot spots. Furthermore, areas of special ecological interest were identified that might be negatively affected by flood events.

5. Results

The results of the flood risk assessment refer to the micro scale level of the study area: Tavira city. Figure 5.18 shows the location of an exemplary result (flood extent for the historical flooded areas) in order to demonstrate the location of the following hazard, danger and risk maps in the whole basin.

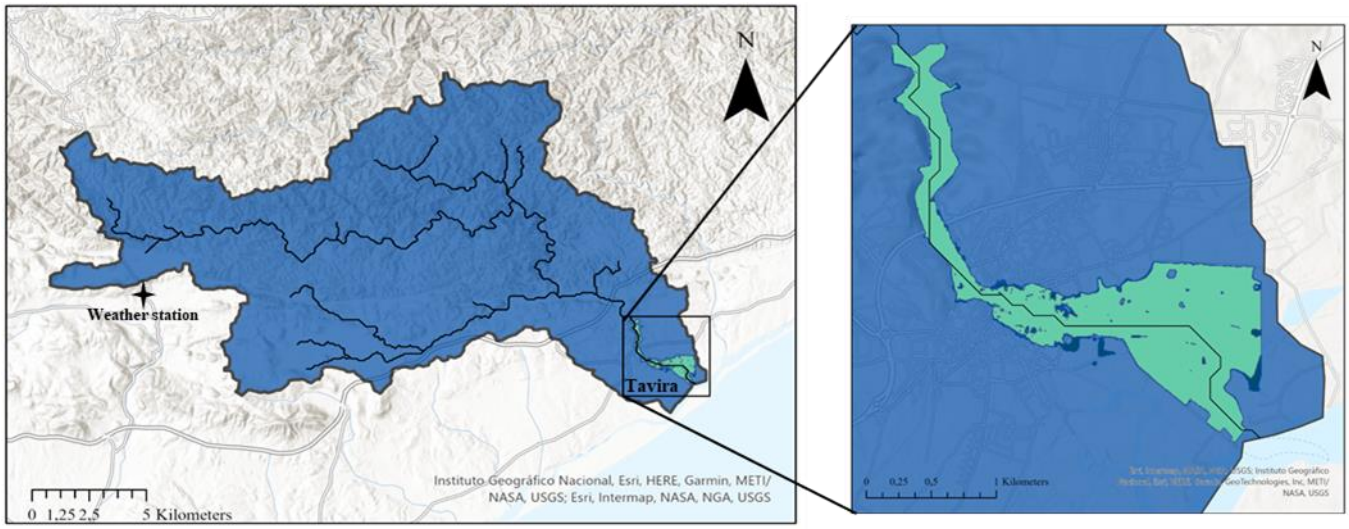

Figure 5.18: Location of the hazard and risk maps in the whole basin.

5. Flood hazard maps

5.1.1 Flood extent maps

Figure 5.19 shows the sizes of the flooded areas for the two historical flood events and the six future flood scenarios in m^2 throughout the time, whereas Figure 5.20 shows the position and geographic spread for the flood scenarios in the study area. In each map the lighter blue represents the floods with return period of 20 years and in darker blue the return period of 100 years. The maps all show similar extents in the northern and eastern part of the flood plain for the different scenarios, while they differ greatly in the south-eastern part. All of them show a greater area in the T100 floods than in the T20 floods and the trend is increasing towards the future. The smallest extent can be found at the T20-historical flood event with an area of 1 723 539 m^2 which is 67% of the greatest extent (2 569 830 m^2) at the T100- long term flood scenario. At the historical events there is an increase in the flood extent from 6.6 % from the T20 event to the T100 event; at the short, mid, and long term there is an increase of 22.9%, 17.9%, and 21.7 %, respectively.

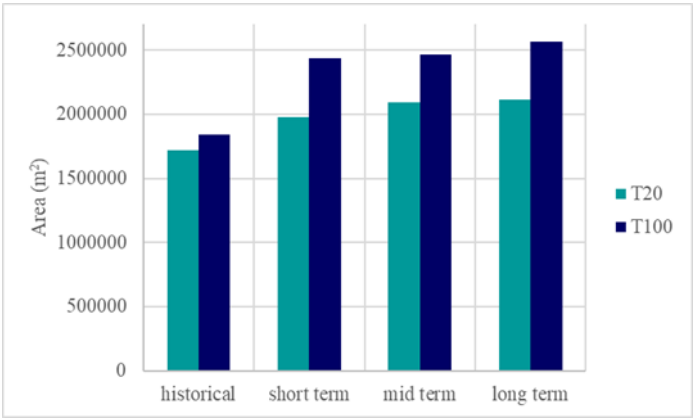

Figure 5.19: Area of the flood extent in the two past flood events (historical) and the future flood scenarios (short, mid, and long term development).

Figure 5.20: Flood extent maps for the two past flood events (historical) and the future flood scenarios (short, mid, and long term development).

5.1.2 Flood depth maps

Figure 5.21 shows the maps of the flood depths in the area of their respective flood extent for the different scenarios. The smallest flood depth ranges from 0 m (in all scenarios) to 8.66 m (T100 long term). The smallest maximum water depth occurs in the T20 historical flood event with a depth of 6.23 m. The highest water depth can be found at the location of the water stream and is then decreasing from there. In the south-eastern part of the three T100 future scenarios, there is an area of the flood plain that is deeper than in the surrounding area. The mean flood depth ranges from 1.3 m (T20 historical) to 1.6 m (T100 long term). The maximum water depths between the two return periods within the same time period range from 11% (historical) to 18% (long term).

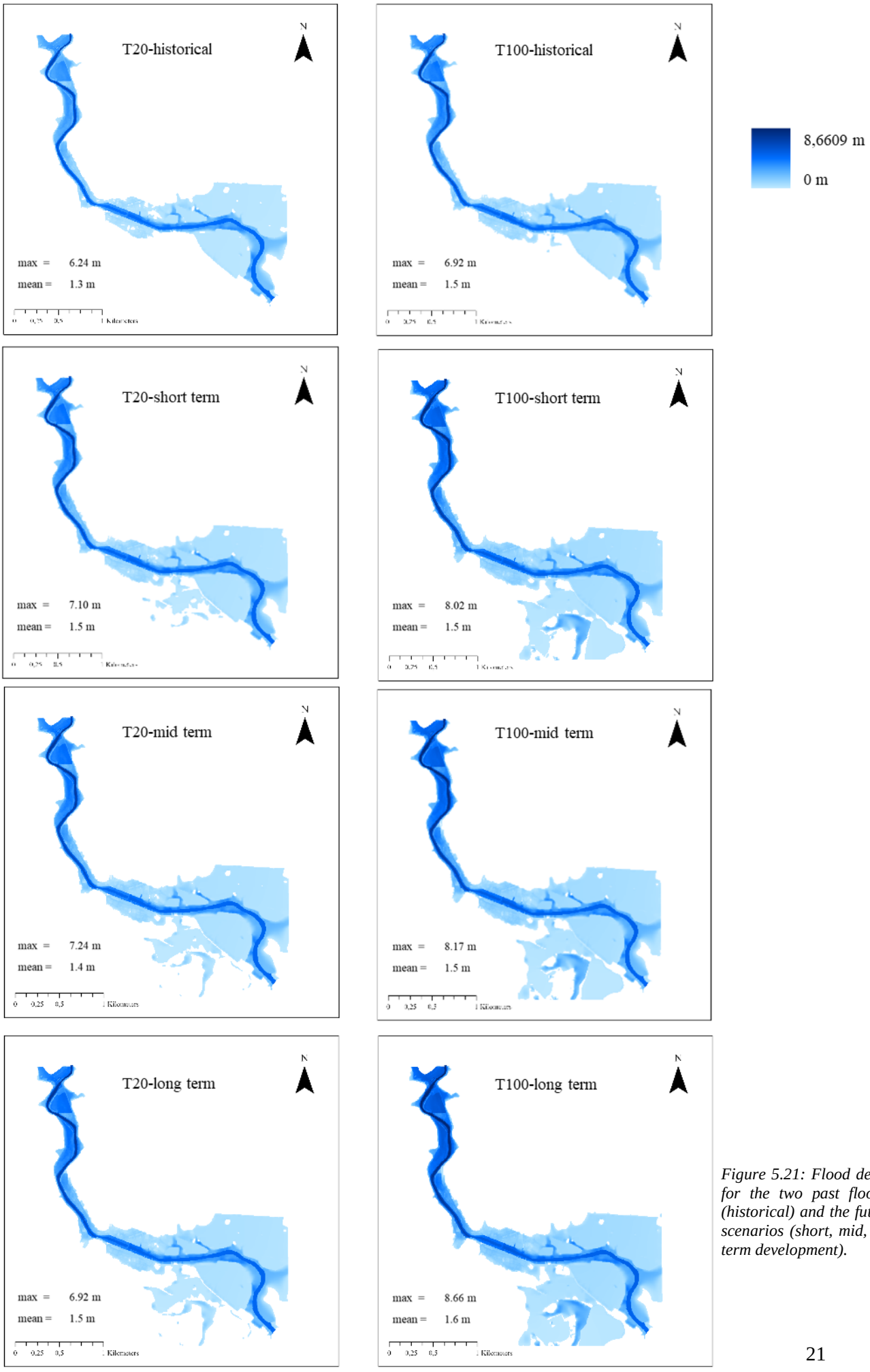

Figure 5.21: Flood depth maps for the two past flood events (historical) and the future flood scenarios (short, mid, and long term development).

5.1.3 Flood velocity maps

The maps of the flood velocity (Figure 5.22) show a similar pattern as the flood depth maps. The highest values can be found at the river course in every flood event and future scenario. The highest velocity occurs at the T100- long term scenario (4.30 m/s). It also has the highest mean flood velocity (0.51 m/s), whereas the smallest mean flood velocity can be found at the T20 historical flood event (0.33 m/s). The percentage increase from the T20 flood scenarios to the T100 flood scenarios is in every case around 10 %, with 14 % at the long term scenario and 10 % at the mid term scenario.

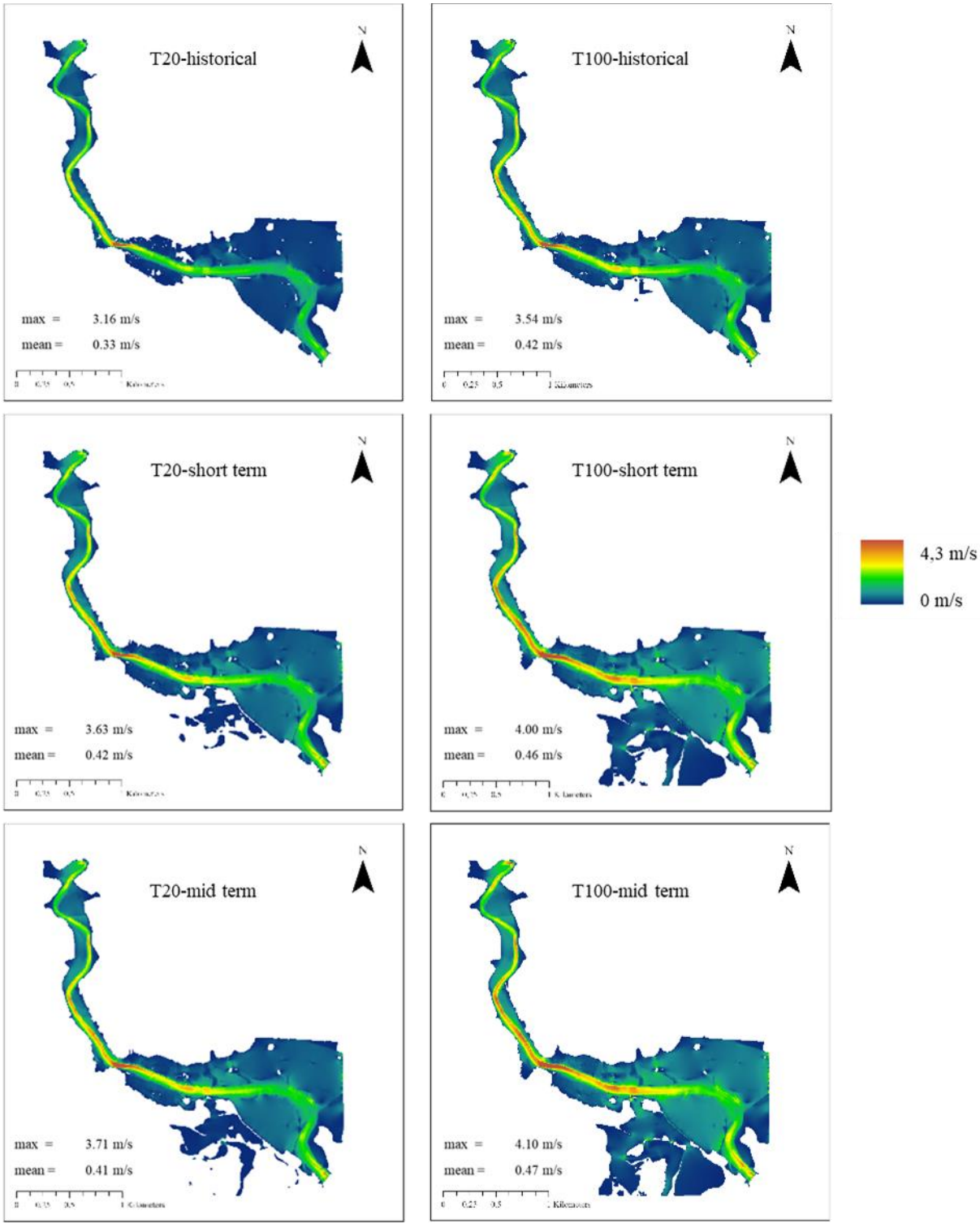

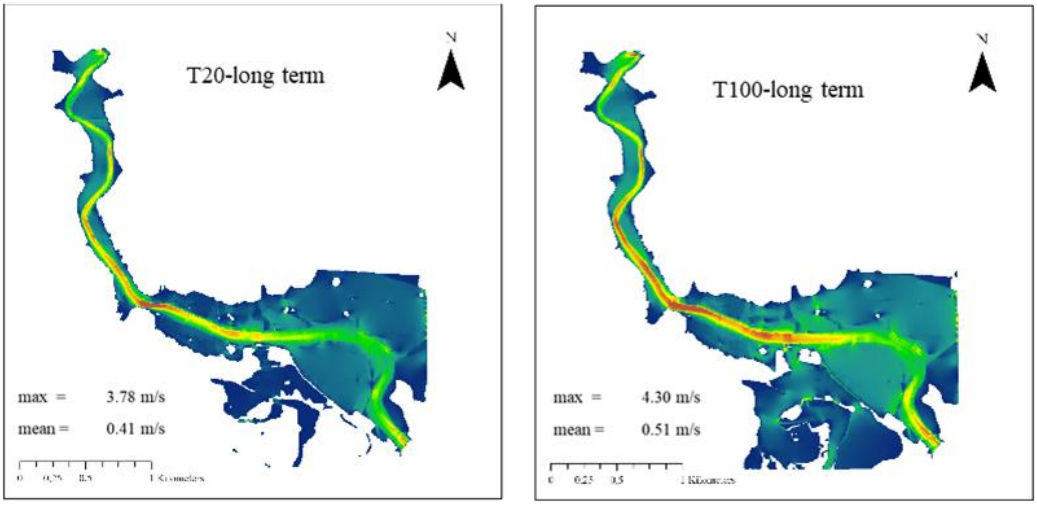

Figure 5.22: Flood velocity maps for the two past flood events (historical) and the future flood scenarios (short, mid, and long term development).

5.2 Flood danger maps

The flood danger maps are a combination of the flood depth and the flood velocity; therefore, they show a similar distribution regarding their severeness as the flood depth and velocity maps. The flood danger was classified as non existent (1), low (2), average (3), high (4) and very high (5). Figure 5.23 shows that the danger is highest at the river course and is decreasing towards the sides. At the T100 future flood scenarios, there is also an area in the south-eastern part of the flood plain that has a higher danger (low to average) than the surrounding area. That phenomena occurred already in the hazard maps. Figure 5.24 gives an overview of the distribution between the different classes in the flooded area. In every past flood event and future scenario class 1 represents the highest share (55-62% of the total area), followed by class 4 (15-17%). Class 2 and 5 have very similar shares in each scenario (5-11%, 4-9% respectively). There is no general trend in increasing the shares of class 4 and 5 from the short term scenarios (T20=16%, 8%; T100=15%, 8% respectively) to the long term scenarios (T20=16%, 8%; T100=15%, 9% respectively).

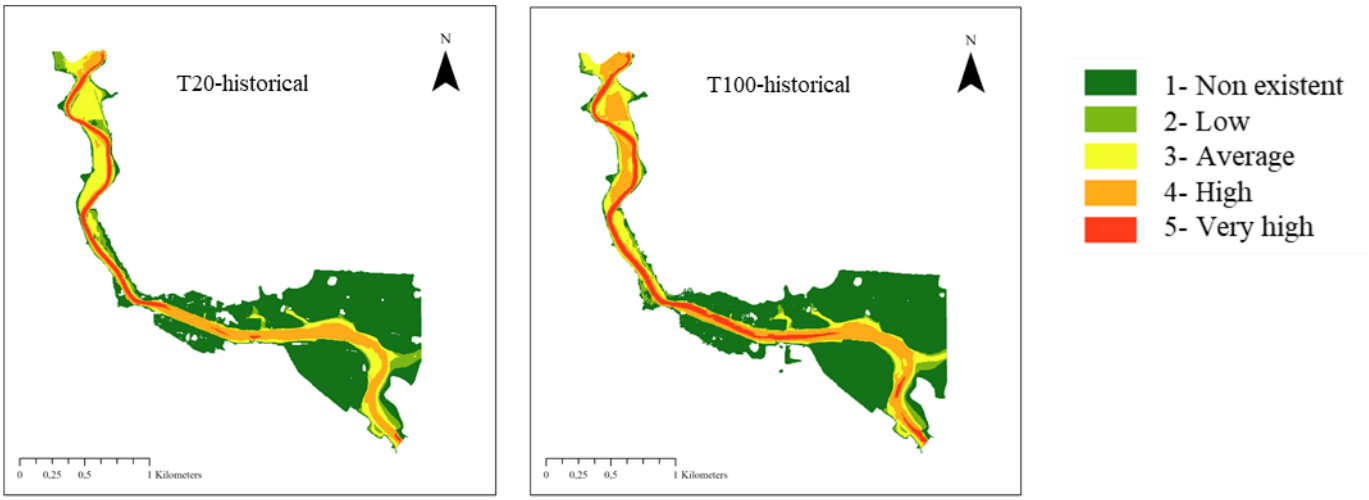

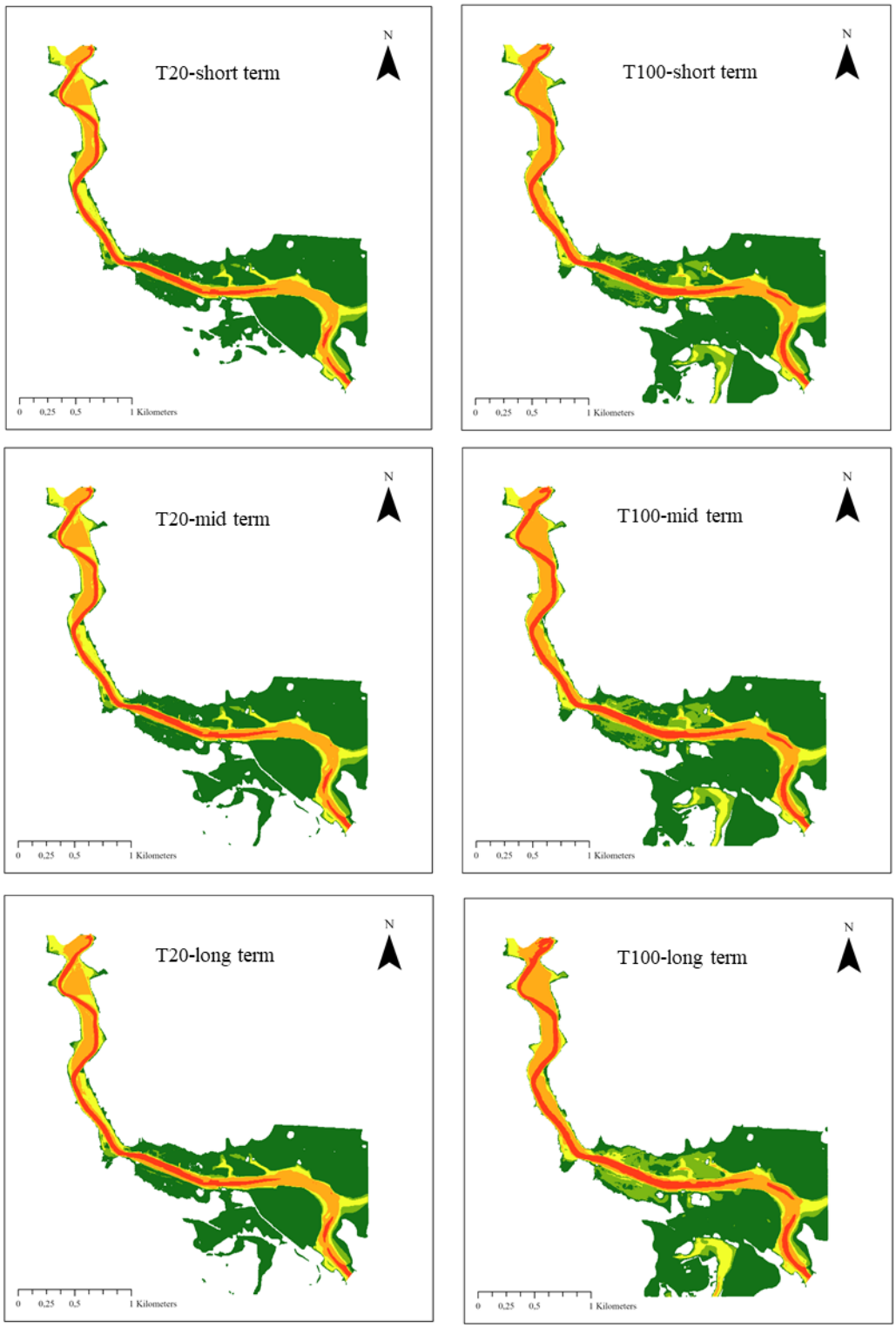

Figure 5.23: Flood danger maps for the two past flood events (historical) and the future flood scenarios (short, mid, and long term development); the danger is presented in five classes: non existent (1,dark green), low (2, light green), average (3, yellow), high (4, orange), very high (5, red).

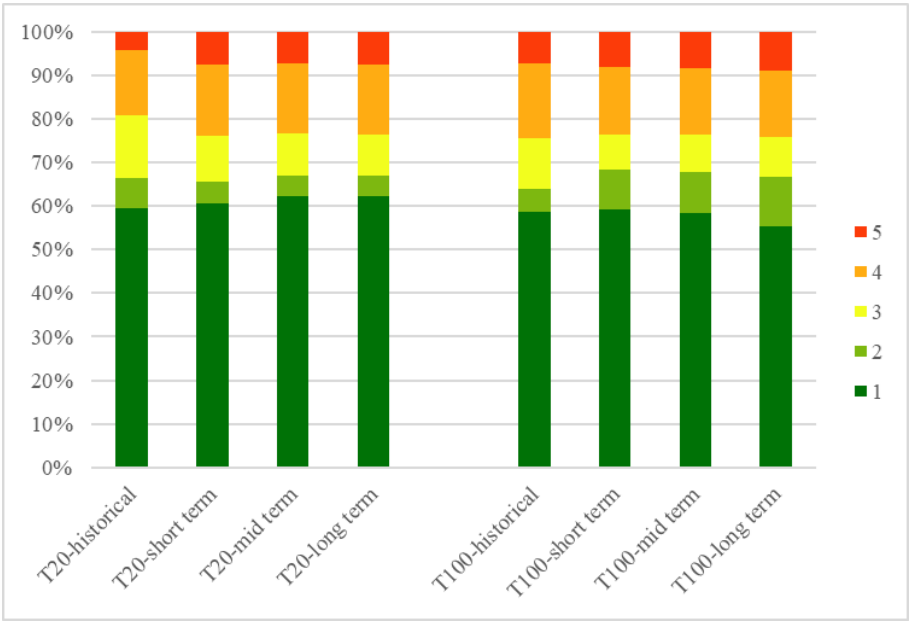

Figure 5.24: The percentages of the five danger classes (1-5) for the eight scenarios.

5.3 Risk maps

Figure 5.25 shows the distribution of the landcover classes Residential, Infrastructure, Industry, Commerce, Agriculture, and Transport. The shares of the four building types are as follows: 56% Residential, 9% Industrial, 38% Commercial, and 0.3% Transport. The commercial buildings can be further divided into Sport (30%), Restaurant (16%), Office (8%), Hotel (15%), Health (2%), General trading (14%), Education (5%), Church and Singular buildings (8%), and Workshop (2%) (Appendix B for the landcover map). The white area in between the different landcover classes is free area that is either sealed or unsealed and not used. This landcover map is the base for the following risk maps.

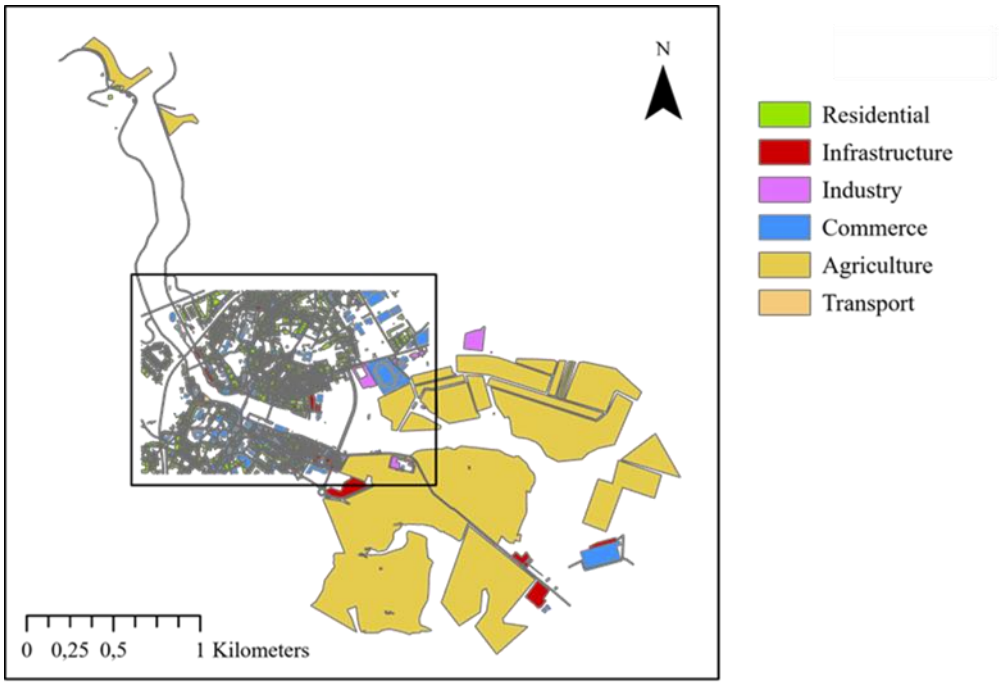

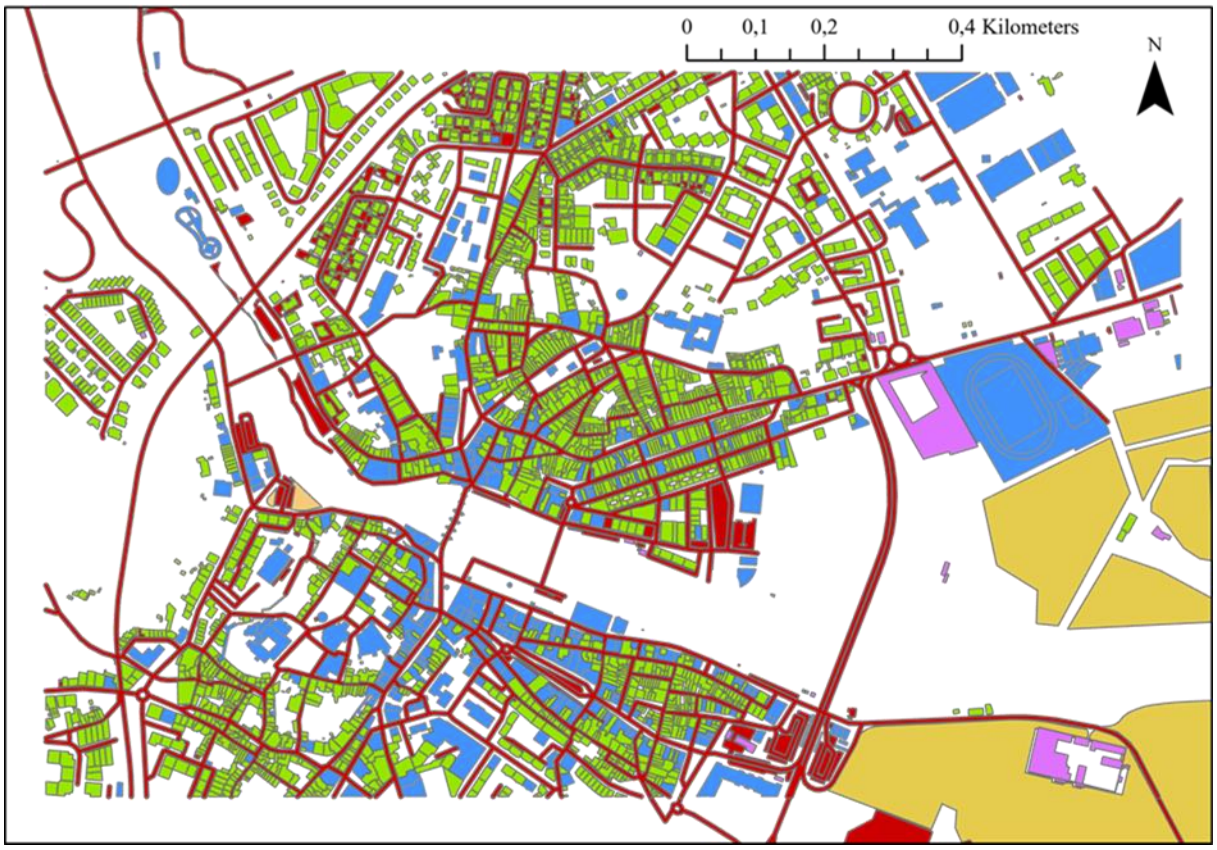

Figure 5.25: Map of the landcover in the six classes: residential, infrastructure, industry, commerce, agriculture, transport.

5.3.1 Economic risk

Absolute economic damage

The absolute economic damage in € per landcover class and per scenario is shown in Figure 5.26 (based on the European depth-damage curve) and Figure 5.27 (based on the adjusted Spanish depth-damage curve). Figure 5.26 shows that the landcover class Commerce and Residential are responsible for the biggest part of the economic damage in every past flood event and future scenario (44-49 % each). The smallest part constitutes the Agriculture land cover class with values lower than 1 % in every scenario (0.09-0.11 %). The other three classes- Industry, Transport, and Infrastructure- all have shares of around 1.4-4.1 %. In total the highest amount of economic damage was calculated for the T100 flood in the long term development (29 million €) which is 4 times more economic damage than in the scenario with the smallest economic damage (T20 historical, 7 million €). By comparing the two return periods in the same time frame, there is an increase in the economic damage from the T20 return period to the T100 return period in every case. The highest can be found at the historical flood event (88 %), followed by the long term development (70%). Both, the short and mid term development show an increase of around 53%.

The absolute economic damage of the land cover class Commerce was also calculated in further segmented classes (Figure 5.27). The figure displays clearly, that in every scenario, the calculated damage based on the adjusted Spanish depth-damage curve is less than the calculated damage based on the European depth-damage curve (blue column on the left from the splited column). Thus, the total economic damage is higher by using the European depth-damage curve. The economic damage based on the European depth-damage curve is between 14 % (T20 long term) and 31 % (T100 historical)

higher than the economic damage based on the adjusted Spanish depth-damage curve. The biggest part of the total economic damage are Restaurants (~39%), followed by General trading (~17%). The smallest share is the landcover class Hotel (~0.86%).

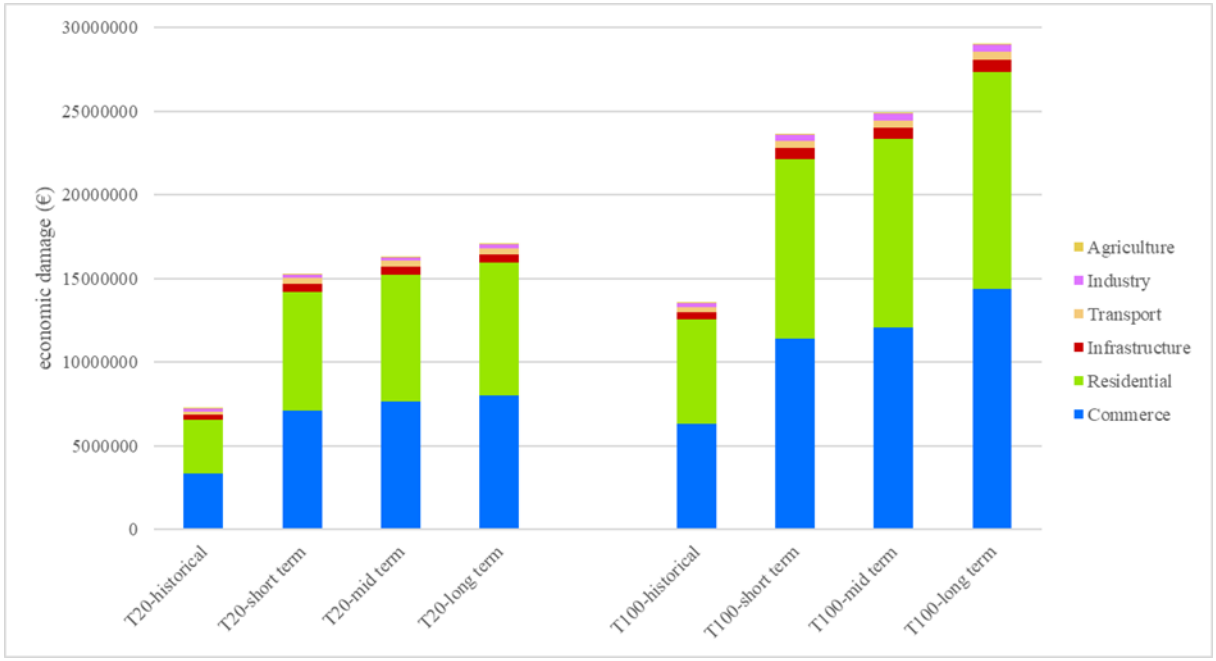

Figure 5.26: Absolute economic damage for the two past flood events (historical) and the future flood scenarios (short, mid, and long term development) divided into the European landcover classes.

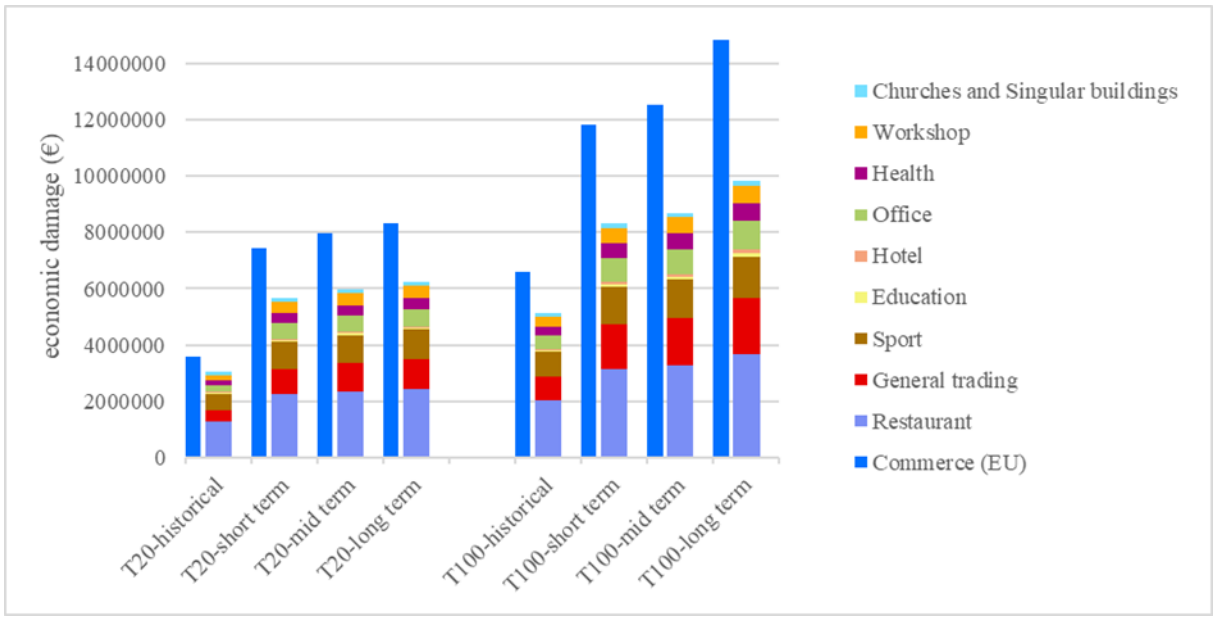

Figure 5.27: Absolute economic damage for the two past flood events (historical) and the future flood scenarios (short, mid, and long term development) divided into the Spanish landcover classes and the European landcover class commerce.

Probability-damage curve

Ideally, probability-damage curves have more than just two probabilities (return periods), but in this work only two probabilities (0.01 (T100), 0.05 (T20)) were available. Figure 5.28 shows the probability-damage curve for the short term development. The probability-damage curves for the mid and long term development can be found in Appendix C. The two points represent the economic damage (in €) with the exceedance probabilities of 0.01 and 0.05 (yellow, green respectively). The hatched area represents the economic risk (=annual average damage).

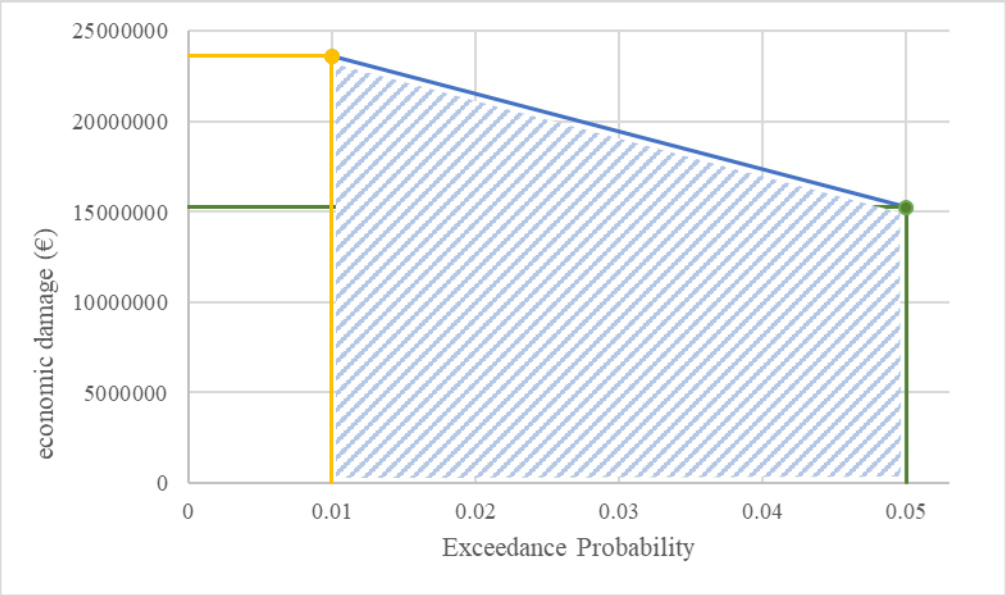

Figure 5.28: Probability-Damage curve for the short term development.

Economic risk (annual average damage)

The annual average damage per time period is shown in Table 5.4. The damage increases from 414 362 € (historical) to 921 513 € (long term).

Table 5.4: Economic risk (annual average damage) in Euro for the historical flood event and the three future flood scenarios (short, mid, and long).

	Economic risk (€)
Historical	414362
Short term	777194
Mid term	823394
Long term	921513

Figure 5.29 shows the distribution of the risk per cell for the short term development (the risk maps for the mid, and long term development can be found in Appendix D), where the risk was standardised between 0 and 10. Table 5.5 shows the risk conversion from the risk per cell in € to a standardised risk value. As the highest risk (10) the highest occurring annual average damage per cell (in €) was used (≤0.085). The highest share is the risk value 0 (~81%), followed by risk value 1 (~10%) and risk value 3 (~4%) in every time frame (see Figure 5.28 and Appendix D). The smallest shares are risk value 8 (~0.004%), risk value 8 (0.003%) and risk value 10 (~0.0006%) in the time frames short, mid, and long term respectively.

Table 5.5: Risk conversion from the risk per cell in € to a standardised risk value (0-10).

Annual average damage (€)	Standardised risk value
≤ 0.0001	0
≤ 0.0085	1
≤ 0.017	2
≤ 0.0255	3
≤ 0.034	4
≤ 0.0425	5
≤ 0.051	6
≤ 0.0595	7
≤ 0.068	8
≤ 0.0765	9
≤ 0.085	10

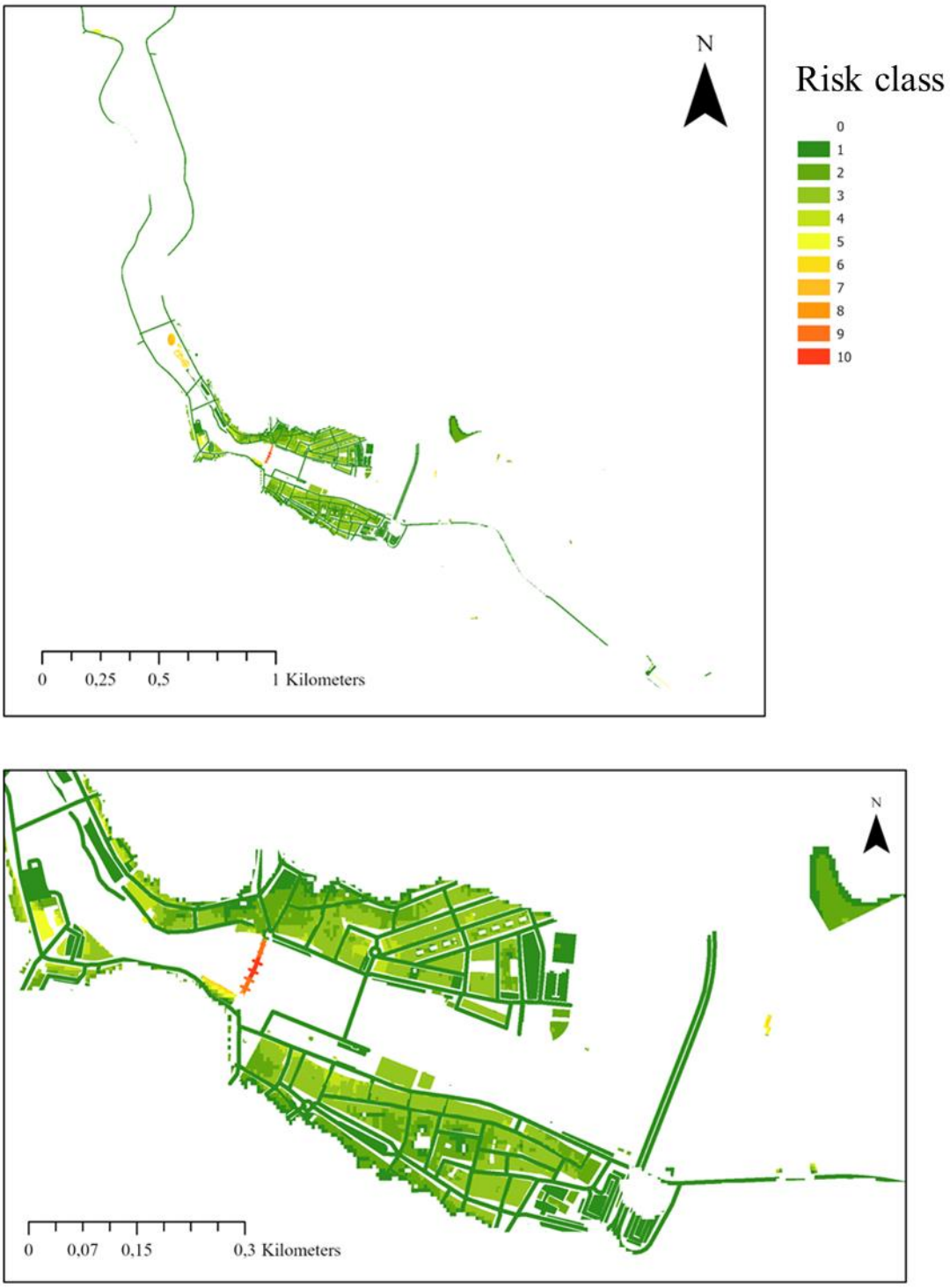

Figure 5.29: Risk map for the short term development with the standardised risk classes (0-10).

5.3.2 Social risk

The population density in the study area is 102 people/km^2 (state 2011). The annual affected population per km^2 (=social risk) and the total affected population is shown in Table 5.6. There is an increase in the total affected population per km^2 as well as in the social risk towards the long term development.

Table 5.6: Total affected population and social risk (annual average affected population) for the historical flood event and the three future flood scenarios (short, mid, and long).

	Total affected population per km2	Social risk
historical	364.0	7.3
Short term	451.5	9.0
Mid term	466.3	9.3
Long term	478.4	9.6

Educational (any kind of schools and kindergartens) and health (hospitals, pharmacies, medical practices) facilities were classified as social hot spots, the location of those are shown in Figure 5.30. For a better orientation, the river course is also shown.

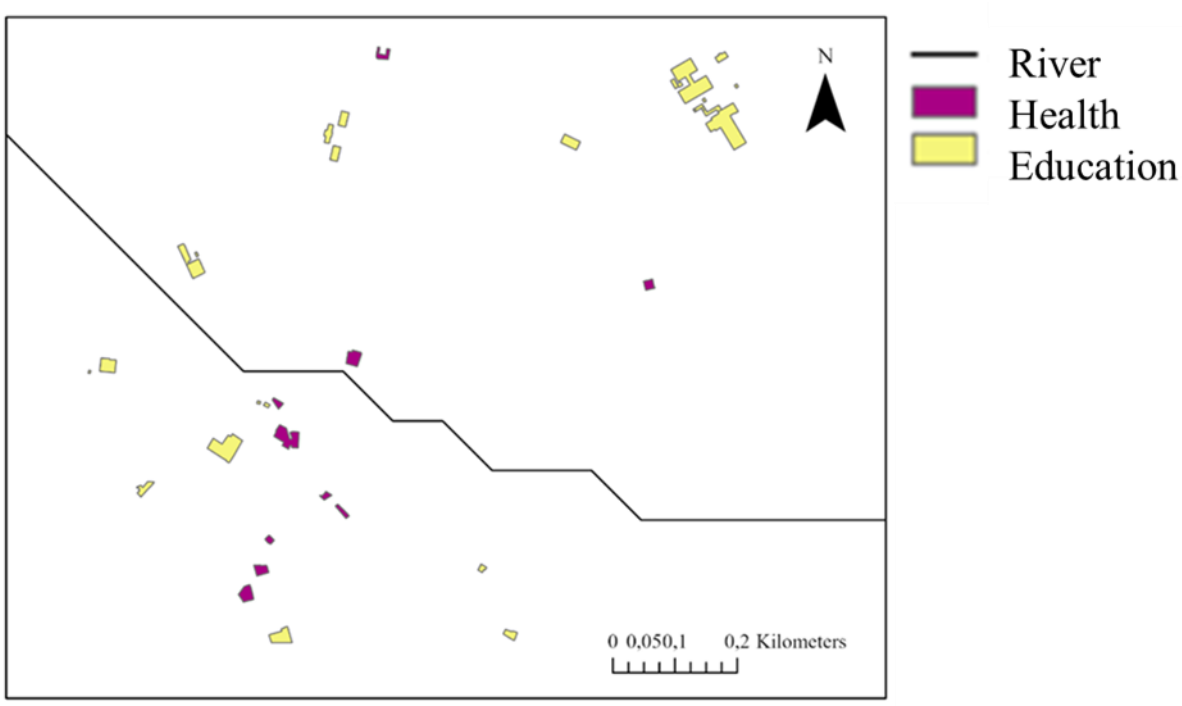

Figure 5.30: Social hotspot in the floodplain area such as schools, kindergartens, hospitals, pharmacies, and medical practices.

Figure 5.31 shows the affected social hotspots. In every scenario (T20 and T100; short, mid, and long term) there were the same facilities affected. The only thing that changed were the extent of the water inside the building, which was disregarded, because in mapping the social risk, it does not matter, compared to the economic risk, what the water depth in the building is or how much it is affected. Affected social hotspots always constitute a risk for more vulnerable people.

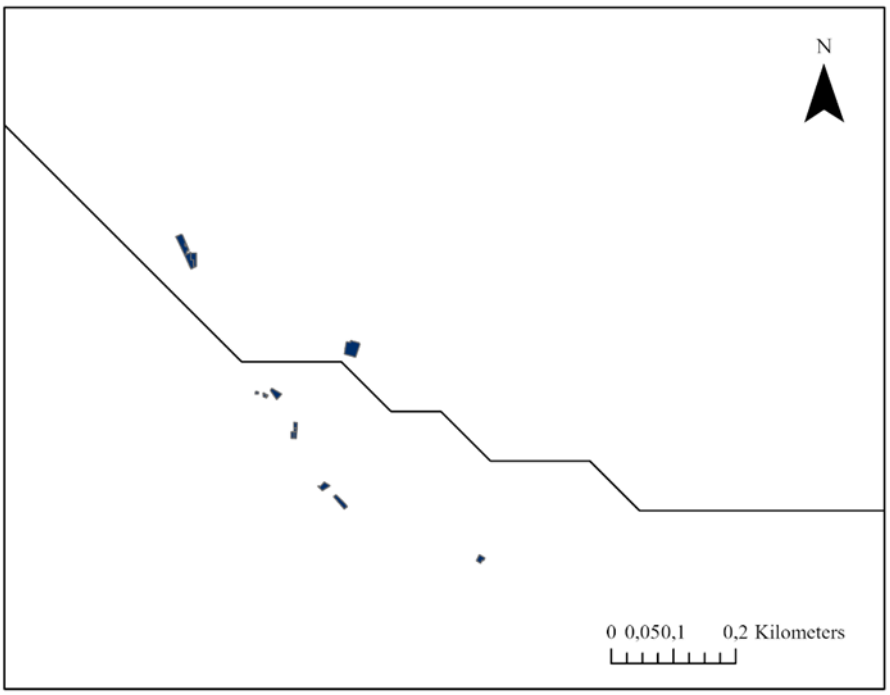

Figure 5.31: Affected social hot spots in both return periods (T20 and T100).

5.3.3 Environmental risk

There were some gas stations, gas and fuel tanks, and a wastewater treatment facility identified as risk for the environment. Like the social hot spots, they were affected in every scenario.

Besides that, the national park Rio Formosa is located at the southern end of the floodplain and therefore affected by the water coming from the city site.

6. Discussion

The obtained results cover the determination of the flood hazard, the flood vulnerability, and the assessment of the associated flood risk in the future. For the future scenarios, the Representative Concentration Pathways (RCP) that shows the highest precipitation in the study area were taken. It was either the RCP4.5 (intermediate-emission scenario) or RCP8.5 (high emission worst case scenario), where the digit represents the radiative forcing in W/m^2 by 2100 compared to the pre-industrial period (1850) (IPCC, 2014). Therefore, for each one of the three future time developments (short, mid, long) the RCP scenario (either RCP4.5 or RCP8.5), that showed the highest peak precipitation for the time period was selected and there was no comparison in the same time period of different climate change scenarios. Since the severeness of extreme precipitation events do not depend on the emission scenario, the difference selections of the RCP scenarios can be explained (Pendergrass et al., 2015). The comparison took place in the two return periods T20 and T100 for each future time period. One clear observation is the increase in the flooded area, maximum water depth, maximum water velocity, and the risk from the T20 to the T100 scenario. Also, there is the same pattern regarding the water depth and the water velocity. Both parameters have their maximum at the river course and decrease with higher distance to the river. Here it is to mention, that the biggest part of the flood occurs mostly in the saline area. Accordingly, the flood danger maps look alike which is obvious because the danger was calculated with those two parameters. Here, it is important to mention that there is no clear trend in an increase of the two highest danger classes (4-high; 5-very high) from the T20 scenario to the T100 scenario. The shares have pretty much the same amount which means that the T100 floods do not necessarily bear a higher danger (if the danger is calculated that way). Only the danger class 1 (non-existent) has in every T20 scenario a higher share than in the T100 scenarios. When it comes to the absolute economic damage, there is again a clear increase from the T20 scenarios to the T100 scenarios with the highest total economic damage in the T100 long term scenario. The increase from the short term scenarios to the long term scenarios depends on the increasing predicted precipitation values as input data for the model. The discrepancy of the absolute economic damages in the landcover class commerce calculated with the Spanish depth-damage curve (the total volume is smaller in every case) can be explained with the different maximum water depths. The European depth-damage curve provides damages for water depths until 6 m, whereas the Spanish depth-damage curve stops at 3 m. Therefore, for water depths higher than 3 m the same damage as for 3 m was used. That will result in an underestimation of the economic risk, in the case of water depths higher than 3 m.

The final calculations and the aim of this thesis include the determination of the economic, social, and environmental risks. The economic risk or the annual average damage was standardised in eleven risk classes. In every scenario the risk class with the lowest share was 0, followed by the risk class 1 which is less than 3.4 $€/m^2$. The risk maps show a similar pattern as the flood hazards maps before. The risk is (within the same landcover class) higher in short distances to the river course. According to the World Bank (2021), Portugal has an average annual flood loss of around 90 million Euro. For the time period 2011-2040, an average annual damage of around 777 thousand Euro for the study area was calculated, what corresponds to around 0.86 % of the average annual damage of whole Portugal.

For the social risk two parameters were calculated: the affected population and the affected hot spots. There is a clear increasing trend from the short term scenario to the long term scenario regarding the annual average affected population, whereas the affected hot spots remain the same, regardless the time frame or return period.

The same result was obtained regarding affected environmental “hot spots”. But in addition to the environmental hot spots, the possible impacts of the flood on the national park Rio Formosa need to be

mentioned. Parts of the Rio Formosa Ramsar site is directly located in the floodplain area and in the area where the flood water will run off. The national park is a complex system of coastal saltwater lagoons and barrier islands. It includes mudflats, sand banks, dune systems, saltmarshes, and Zostera beds. The area has a great importance regarding birds (breeding, hibernation) and the flora (several endemic plants) (Ramsar Convention, 1992). In general, wetlands are areas that either are saturated or flooded permanently or seasonally, so one could think flooding is part of the natural processes and does not bring harm. But concerning floods with water coming from urban and agricultural areas it may be different, even though they are considered as filters for waste, e.g., pollutants from pesticides, industry, and mining such as heavy metals and toxins. The harmful substances can be absorbed by wetland sediments, plants and marine life (Ramsar Convention, 2010). But pollution is one of the environmental impact factors with adverse consequences for wetlands, besides human intrusion and disturbance through e.g., energy production and mining. It can lead to, e.g., wetland ecosystem degradation and species invasion. Therefore, the pollution amount that enters a wetland should be strictly controlled. Climate change and pollution are stated as the greatest impact on marine and coastal wetlands (Xu et al., 2019). Both impact factors are related to floods. The pollution amount stemming from floods can hardly be controlled or managed. Whereas it is likely that the frequency and intensity of floods will increase in the future. So, both impacts can endanger the wetland ecosystem located in the floodplain.

Uncertainties in the methodology occur in every step of the flood risk assessment from the source and pathway (hydrological modelling) to the receptors (landcover) and consequences (depth-damage curve, etc.) (Beven et al., 2014). Bruno Merz & Thieken (2009) distinguish between aleatory and epistemic uncertainties. Aleatory uncertainties originate from the variability and natural changes in the study area, e.g., changes in land use and the according changes in runoff or infiltration capacity. On the other hand, epistemic uncertainties arise from an absence of knowledge about the study area, e.g., the exact damage value of a building. The differentiation of those two uncertainties is mainly important when trying to reduce uncertainties. The aleatory uncertainties usually cannot be reduced, whereas epistemic ones can be reduced. It is also important to mention that there is no clear line between those uncertainties. When speaking about uncertainties in climate change impact assessments, the cascade of uncertainties is often mentioned. This cascade includes uncertainties in climate models, impact models, and damage cost models. The understanding and acknowledgment of this “cascade” helps to reduce uncertainties in the risk assessment process by e.g., weighing the severity of the single factors regarding their relevance for decision makers (Halsnæs & Kaspersen, 2018).

The uncertainties start with the hazard maps, the information about the flood area extent, the flood depth, and the flood velocity are all based on hydrological modelling. Here again, the input data for the flood modelling is based on calculations and predictions about how the precipitation might look like in the future.

In order to include more flood parameters than only the flood depth, flood danger maps can be used to reduce uncertainties in the risk evaluation. They are a combination of different flood parameters. In this thesis, the flood velocity was combined with the flood depth. The consideration of other flood parameters can be crucial in calculating the risk properly. For example, the damage to agricultural areas is mostly more dependent on the time of the year the flooding occurs and the duration of the flood than the flood depth (Forster et al., 2008). Since in this study area mainly urban areas were affected, the time of the season would not have that much effect on the economic risk. But considering that Tavira is a very touristic city, the social risk could be different during the year.

Next, the exposure or vulnerability can change in the future. The exposure and vulnerability of the elements at risk are based on the current land cover. In the future it is likely that the landcover in the study area will change and thereby also the risk. Figure 6.32 shows the land use change from the year 1990 to the year 2018 in ha. There is especially an increase in the artificial surfaces (Discontinuous urban fabric, Industrial or commercial units, Mineral extraction sites), the permanent crops (Fruit trees and berry plantations, Olive groves) and Shrub and/or herbaceous vegetation associations (Sclerophyllous vegetation, Transitional woodland-shrub) and a decrease in Heterogeneous agricultural areas (Annual crops associated with permanent crops, Complex cultivation patterns, Land principally occupied by agriculture, with significant areas of natural vegetation, Agro-forestry areas) and (Forests Broad-leaved forest, Coniferous forest, Mixed forest) (Land use maps of the years 1990, 2000, 2006, 2012 and 2018 can be found in Appendix E). Land use changes can result in an increased risk of floods. Here especially urbanisation, deforestation and cultivation are contributing factors. Several different mechanisms such as reduced infiltration rate and capacity or lower soil porosity are accompanied with those changes (Tollan, 2002). This transformation already occurred in the study area in the past and it is likely that this process will go on in the future.

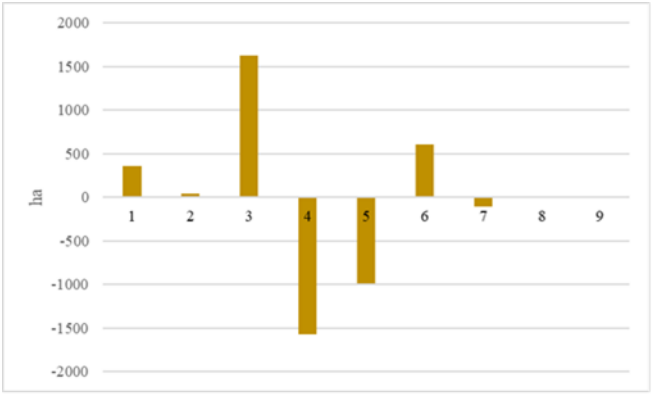

1	Artificial surfaces
2	Arable land
3	Permanent crops
4	Heterogeneous agricultural areas
5	Forest
6	Shrub and/or herbaceous vegetation associations
7	Open spaces with little or no vegetation
8	Coastal wetlands
9	Marine waters

Figure 6.32: Land use change from the year 1990 to the year 2018.

The classification of the landcover classes also has an impact on the occurring damage. In the literature there are different proposals for the classification. In this thesis it was classified in terms of the business sector. Other classification parameters could have been the building type or the building material. The building type can have a major influence on the amount of damage, e.g., a building with just one floor is more affected than a building with multiple floors. The material also influences the damage, e.g., the total weight of the building or the drying rate of the building (Merz et al., 2010). The decision of the classification type is often limited due to the existence of fitting depth-damage curves. Regarding the social risk, or rather the annual affected population, the same problem as with the landcover can be found. The population data is based on information from 2011 and it is likely that it will change in the future and even possibly vary greatly during the year.

Besides the change in the landcover it is also important to recognise, that the susceptibility of those elements at risk, are counted as equal within their landcover class. But in reality, e.g., not every industrial building undergoes the same monetary damage. This assumption or generalisation can lead to either an over- or underestimation of the economic risk. In addition, the use of depth-damage curves only takes into account the hazard flood depth and does not consider, e.g., flood velocity or the duration of the inundation (de Moel & Aerts, 2011). Another uncertainty regarding depth-damage curves is their limitation in the used maximum water depth. In this thesis, e.g., the maximum water depth was 8.6 m, but the European depth-damage curve provides only damage values until 6 m and for the Spanish one

even just 3 m. Therefore, all flood depth values higher than 3 or 6 m (depending on the curve) were probably underestimated.

As one of the biggest parts of uncertainties, the calculation of the economic risk (=average annual damage) has to be named. It is based on damage-probability curves, which in this case only consist of two known data points (exceedance probabilities of 0.005 and 0.001(T20 and T100 floods)). Since the definition of the risk is expressed as the "area under the curve", it is ideal to have as many data points as possible to display the curve as exact as possible. Figure 6.33 shows a comparison between the constructed probability-damage curve based on the obtained results in this thesis (left) and one with more data points (right). The more data points there are the better pictured is the risk. The comparison shows that the risk is likely overestimated with just the two data points, because when there are only two points known – that also have a lot of missing data points in between- the curve displays a linear line between those two. According to Ward et al. (2011) the calculated risk based on three return periods (low, medium, and high probability) is already overestimated by 33-100 %. Consequently, using just two return periods the overestimating has an even higher degree in this thesis.

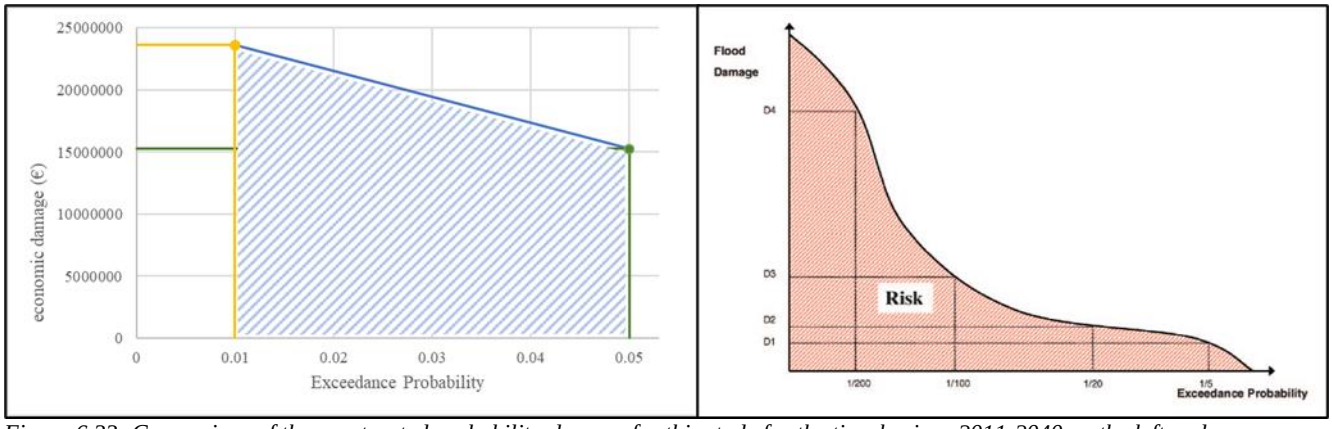

Figure 6.33: Comparison of the constructed probability-damage for this study for the time horizon 2011-2040 on the left and a more ideal probability-damage curve with more data points from (Meyer et al., 2009).

There is not only arising uncertainties with just two data points but also in the selection of the lowest exceedance probability and the highest. As an example, taking a 10-year return period as lowest return period (instead of a zero-damage point) already leads to an underestimation of 33%. Even though floods with a relatively high return period (= low exceedance probability) lead to higher economic damages does not mean they are more important to consider in the risk assessment. Floods with low return periods (=high exceedance probabilities) may lead to a lower economic damage, but their higher frequency makes them as important as the floods with high economic damage (P. J. Ward et al., 2011).

All these calculation steps and assumptions contain at least a certain degree of uncertainty which then accumulates in the final calculation of the risk.

7. Conclusion

Overall, the obtained results show an increase in the economic flood risk in the future due to changing rainfall patterns in climate change scenarios. Regarding the social and environmental risk there was no distinct difference in the scenarios except the annual average affected population. Here an increase during the years can also be observed. The flood risk for the future time periods was calculated with modelled extreme precipitation values either from RCP4.5 or RCP8.5 scenario. The RCP scenario with the higher precipitation was selected. For each time period, two flood events with the return period of 20 and 100 years were observed. Besides the increase of the economic risk during the time, there is a clear increase from the T20 flood scenarios to the T100 flood scenarios regarding not only the risk itself but also the flood extent, the maximum flood depth, the flood velocity, and the flood danger. The calculation was based on depth-damage curves provided by the European Commission and has a maximum water depth of 6 m. The economic risk is often expressed as the average annual damage. For the time period 2011-2040, the annual average damage is around 777 thousand Euro, what is around 0.86% of the annual average damage of whole Portugal according to the World Bank (2021).

During the process of calculating the economic risk, uncertainties arised. They can be found in almost every step of the methodology: the input data for the modelled floods are based on modelled precipitation data and the current land cover; the economic damage is only calculated based on the flood depth other flood parameters were not included such as the flood velocity, debris, or the season the flood occurs; the classification of the landcover has to make compromises due to the limitation of the land cover classes covered in the available depth-damage curves; the landcover is likely to change in the future mainly due to urbanisation; the calculation of the annual average damage is based on damage-probability curves, which have a higher accuracy the more return periods (probabilities) are included. Partly the uncertainties can be measured and the over- or underestimation can be addressed. For example, more exceedance probabilities could be included to get an annual average damage with a higher confidence. But some uncertainties are just based on models that always are accompanied with a degree of uncertainty. Also, there is no way of knowing how the landcover will look in the future.

In addition to the increase in extreme precipitation in the future, increased hydrophobicity of the soils in the future due to droughts and sealing of land due to urbanisation will promote floods and therefore increase the flood risk. This interaction between floods and droughts will get more and more important in the future and is particularly critical in the Algarve region since even though the event of extreme precipitation events with a great water volume will increase, the general precipitation amount decreases. It is important to be aware of the uncertainties arising during the applied methodology. Nevertheless the uncertainties and limitations, the assessment of flood risk is an important part of dealing with natural hazards in the future and it gives a distinct necessity of taking actions in order to protect the population and their belongings.

8. References

APA, 2015. Flood Risk Management Plan: Hydrographic Region 8 - Ribeiras do Algarve (1st Cycle)

Bebianno, M. J. (1995). Effects of pollutants in the Ria Formosa Lagoon, Portugal. *Science of the Total Environment*, *171*(1–3), 107–115. https://doi.org/10.1016/0048-9697(95)04672-9

Beisecker, D. R., Dießelberg, F., Dr. Stephan Hannappel Theresa, S., Senoner, F., Strom, A., & Zettl, E. (2020). *Veränderungen der Wasseraufnahme und -speicherung landwirtschaftlicher Böden und Auswirkungen auf das Überflutungsrisiko durch zunehmende Stark- und Dauerregenereignisse*.

Beven, K., Leedal, D., McCarthy, S., Lamb, R., Hunter, N., Keef, C., Bates, P., Neal, J., & Wicks, J. (2014). Framework for assessing uncertainty in fluvial flood risk mapping. *Flood Risk Management Research Consortium Research Report, June*. www.ciria.org%0Awww. floodrisk. org. uk

Bokwa, A. (2013). Natural Hazard. In P. T. Bobrowsky (Ed.), *Encyclopedia of Natural Hazards. Encyclopedia of Earth Sciences Series*. Springer, Dordrecht.

Costa, A. C., Santos, J. A., & Pinto, J. G. (2012). Climate change scenarios for precipitation extremes in Portugal. *Theoretical and Applied Climatology*, *108*(1–2), 217–234. https://doi.org/10.1007/s00704-011-0528-3

CRED, & UNISDR. (2015). *The Human Cost of Weather Related Disasters - 1995 - 2015*. https://doi.org/10.13140/RG.2.2.17677.33769

de Moel, H., & Aerts, J. C. J. H. (2011). Effect of uncertainty in land use, damage models and inundation depth on flood damage estimates. *Natural Hazards*, *58*(1), 407–425. https://doi.org/10.1007/s11069-010-9675-6

Dias, L., Braunschweig, F., Grosso, N., Costa, H., & Garrett, P. (2014). *Flood Risk Mapping – Methodological Guide*. 77. https://www.researchgate.net/publication/280564924_Flood_Risk_Mapping_-_Methodological_Guide

[DVWK] Deutscher Verband für Wasserwirtschaft und Kulturbau. (1985). Ökonomische Methoden von Hochwasserschutzwirkungen. Arbeitsmaterialien zum methodischen Vorgehen. In: DVWK-Mitteilungen. Bonn (DE): DVWK.

[EC] European Commission. (2007). Directive 2007/60/EC of the European Council and European Parliment of 23 October 2007 on the assessment and management of flood risks. *Official Journal of the European Union, OJ L 288*, 27–34. http://eur-lex.europa.eu/legal-content/EN/TXT/PDF/?uri=CELEX:32007L0060&from=EN

[EEA] European Environmental Agency. (2017). *Climate change, impacts and vulnerability in Europe 2016 - An indicator-based report* (Issue 1). https://www.eea.europa.eu/publications/climate-change-adaptation-and-disaster

Ferreira, A., Oliveira, A., Dias, L. F., Fernandes, L., Brito, D., Braunschweig, F., Sampath, R., Moura, D., Mendes, I., Carrasco, A. R., Costas, S., & C. Veiga-Pires, C. (2019). *Relatório setor segurança de pessoas e bens: vulnerabilidades atuais e futuras*.

Forster, S., Kuhlmann, B., Lindenschmidt, K. E., & Bronstert, A. (2008). Assessing flood risk for a rural detention area. *Natural Hazards and Earth System Science*, *8*(2), 311–322. https://doi.org/10.5194/nhess-8-311-2008

Foudi, S., Osés-Eraso, N., & Tamayo, I. (2015). Integrated spatial flood risk assessment: The case of Zaragoza. *Land Use Policy*, *42*(March 2018), 278–292.

https://doi.org/10.1016/j.landusepol.2014.08.002

Guadiana, D. (2020). *Cartas de Zonas Inundáveis e Cartas de Riscos de Inundações*.

Guerreiro, S. B., Dawson, R. J., Kilsby, C., Lewis, E., & Ford, A. (2018). Future heat-waves, droughts and floods in 571 European cities. *Environmental Research Letters*, *13*(3). https://doi.org/10.1088/1748-9326/aaaad3

Halsnæs, K., & Kaspersen, P. S. (2018). Decomposing the cascade of uncertainty in risk assessments for urban flooding reflecting critical decision-making issues. *Climatic Change*, *151*(3–4), 491–506. https://doi.org/10.1007/s10584-018-2323-y

Hov, Ø., Cubasch, U., Fischer, E., Höppe, P., Iversen, T., Kvamstø, N. G., Kundzewicz, Z. W., Rezacova, D., Rios, D., Santos, F. D., Schädler, B., Veisz, O., Zerefos, C., Benestad, R., Murlis, J., Donat, M., Leckebusch, G. C., & Ulbrich, U. (2013). *Extreme Weather Events in Europe :* (Issue October).

Huizinga, J., de Moel, H., & Szewczyk, W. (2017). Global flood depth-damage functions. Methodology and the database with guidelines. In *Joint Research Centre (JRC)*. https://doi.org/10.2760/16510

IPCC. (2014). *Climate Change 2014: Synthesis Report. Contribution of Working Groups I, II and III to the Fifth Assessment Report of the Intergovernmental Panel on Climate Change* (R. K. Pachauri & L. A. Meyer (eds.)).

Klijn, F. (2009). Flood risk assessment and flood risk management: An introduction and guidance based on experiences and findings of FLOODsite. *FLOODsite Deltares, Delft Hydraulics, Delft, the Netherlands*, 143.

Kottek, M., Grieser, J., Beck, C., Rudolf, B., & Rubel, F. (2006). World map of the Köppen-Geiger climate classification updated. *Meteorologische Zeitschrift*, *15*(3), 259–263. https://doi.org/10.1127/0941-2948/2006/0130

Martínez-Gomariz, E., Forero-Ortiz, E., Guerrero-Hidalga, M., Castán, S., & Gómez, M. (2020a). Flood depth-damage curves for Spanish urban areas. *Sustainability*, *12*(7), 2666. https://doi.org/10.3390/su12072666

Martínez-Gomariz, E., Forero-Ortiz, E., Guerrero-Hidalga, M., Castán, S., & Gómez, M. (2020b). Flood depth-damage curves for Spanish urban areas. *Sustainability (Switzerland)*, *12*(7), 1–25. https://doi.org/10.3390/su12072666

Merz, B., Kreibich, H., Schwarze, R., & Thieken, A. (2010). Review article "assessment of economic flood damage." *Natural Hazards and Earth System Science*, *10*(8), 1697–1724. https://doi.org/10.5194/nhess-10-1697-2010

Merz, Bruno, & Thieken, A. H. (2009). Flood risk curves and uncertainty bounds. *Natural Hazards*, *51*(3), 437–458. https://doi.org/10.1007/s11069-009-9452-6

Meyer, V., Scheuer, S., & Haase, D. (2009). A multicriteria approach for flood risk mapping exemplified at the Mulde river, Germany. *Natural Hazards*, *48*(1), 17–39. https://doi.org/10.1007/s11069-008-9244-4

Pachauri, R. K., Allen, M. R., Barros, V. R., Broome, J., Cramer, W., Christ, R., Church, J. a., Clarke, L., Dahe, Q., Dasgupta, P., Dubash, N. K., Edenhofer, O., Elgizouli, I., Field, C. B., Forster, P., Friedlingstein, P., Fuglestvedt, J., Gomez-Echeverri, L., Hallegatte, S., … van Ypersele, J.-P. (2014). IPCC, 2014. *CLIMATE CHANGE 2014 Synthesis Report*. https://doi.org/10.1017/CBO9781139177245.003

Pendergrass, A. G., Lehner, F., Sanderson, B. M., & Xu, Y. (2015). Does extreme precipitation intensity

depend on the emissions scenario? *Geophysical Research Letters*, *42*(20), 8767–8774. https://doi.org/10.1002/2015GL065854

Ramsar Convention. (1992). *Ramsar information sheet Nr.PT212RIS*.

Ramsar Convention. (2010). *Wetlands: why should I care ? Why is this such an alarming trend ? And why are wetlands actually essential to sustainable development for the human race ?* www.ramsar.org

Região de Turismo do Algarve. (2013). *Tavira*.

Samuels, P., & Gouldby, B. (2009). Languages of Risk: Project definitions. *Genes and the Bioimaginary*, *T32-04–01*. https://doi.org/10.4324/9781315584294-2

Schanze, J. (2006). Flood Risk Management- A basic framework. In *Flood Risk Management: Hazards, Vulnerability and Mitigation Measures*. Springer. http://www.preventionweb.net/english/professional/publications/v.php?id=1068%0Ahttp://www.ncbi.nlm.nih.gov/pubmed/21605785

Tollan, A. (2002). Land-use change and floods: What do we need most, research or management? *Water Science and Technology*, *45*(8), 183–190. https://doi.org/10.2166/wst.2002.0176

UN HABITAT. (2011). Cities and Climate Change: Global Report on Human Setttlements 2011. In *Cities and Climate Change*. https://doi.org/10.1596/978-0-8213-8493-0

Ward, P. J., De Moel, H., & Aerts, J. C. J. H. (2011). How are flood risk estimates affected by the choice of return-periods? *Natural Hazards and Earth System Science*, *11*(12), 3181–3195. https://doi.org/10.5194/nhess-11-3181-2011

Ward, Philip J., de Ruiter, M. C., Mård, J., Schröter, K., Van Loon, A., Veldkamp, T., von Uexkull, N., Wanders, N., AghaKouchak, A., Arnbjerg-Nielsen, K., Capewell, L., Carmen Llasat, M., Day, R., Dewals, B., Di Baldassarre, G., Huning, L. S., Kreibich, H., Mazzoleni, M., Savelli, E., … Wens, M. (2020). The need to integrate flood and drought disaster risk reduction strategies. *Water Security*, *11*(2020). https://doi.org/10.1016/j.wasec.2020.100070

World Bank. (2021). *Financial Risk and Opportunities to Build Resilience in Europe*. https://doi.org/10.1596/35685

Xu, T., Weng, B., Yan, D., Wang, K., Li, X., Bi, W., Li, M., Cheng, X., & Liu, Y. (2019). Wetlands of international importance: Status, threats, and future protection. *International Journal of Environmental Research and Public Health*, *16*(10). https://doi.org/10.3390/ijerph16101818

9. Appendix

Appendix A- fractional functions for the landcover classes

	Residential		**Commercial**		**Industrial**		**Agriculture**		**Infrastructure**		**Transport**	
flood depth (m)	Damage fraction	€/m2	Damage fraction	€/m2	Damage fraction	€/m2	Damage fraction	€/m2	Damage fraction	€/m2	Damage fraction	€/m2
0	0	0	0	0	0	0	0	0	0	0	0	0
0.5	0.25	154.4195	0.15	130.6297	0.15	108.0162	0.3	0.028981	0.25	3.329912	0.316667	124.3722
1	0.4	247.0711	0.3	261.2595	0.27	194.4292	0.55	0.053131	0.42	5.594251	0.541667	212.7419
1.5	0.5	308.8389	0.45	391.8892	0.4	288.0433	0.65	0.062791	0.55	7.325806	0.701667	275.5826
2	0.6	370.6067	0.55	478.9757	0.52	374.4563	0.75	0.072452	0.65	8.65777	0.831667	326.6406
3	0.75	463.2584	0.75	653.1486	0.7	504.0758	0.85	0.082112	0.8	10.65572	1	392.7542
4	0.85	525.0262	0.9	783.7784	0.85	612.092	0.95	0.091772	0.9	11.98768	1	392.7542
5	0.95	586.794	1	870.8649	1	720.1083	1	0.096602	1	13.31965	1	392.7542
6	1	617.6778	1	870.8649	1	720.1083	1	0.096602	1	13.31965	1	392.7542

Table 9.7: Damage functions for the creation of the depth-damage curves for the six land cover classes from (Huizinga et al., 2017).

Appendix B- Landcover accroding to the landcover classes based on the Spanisch depth-damage curve

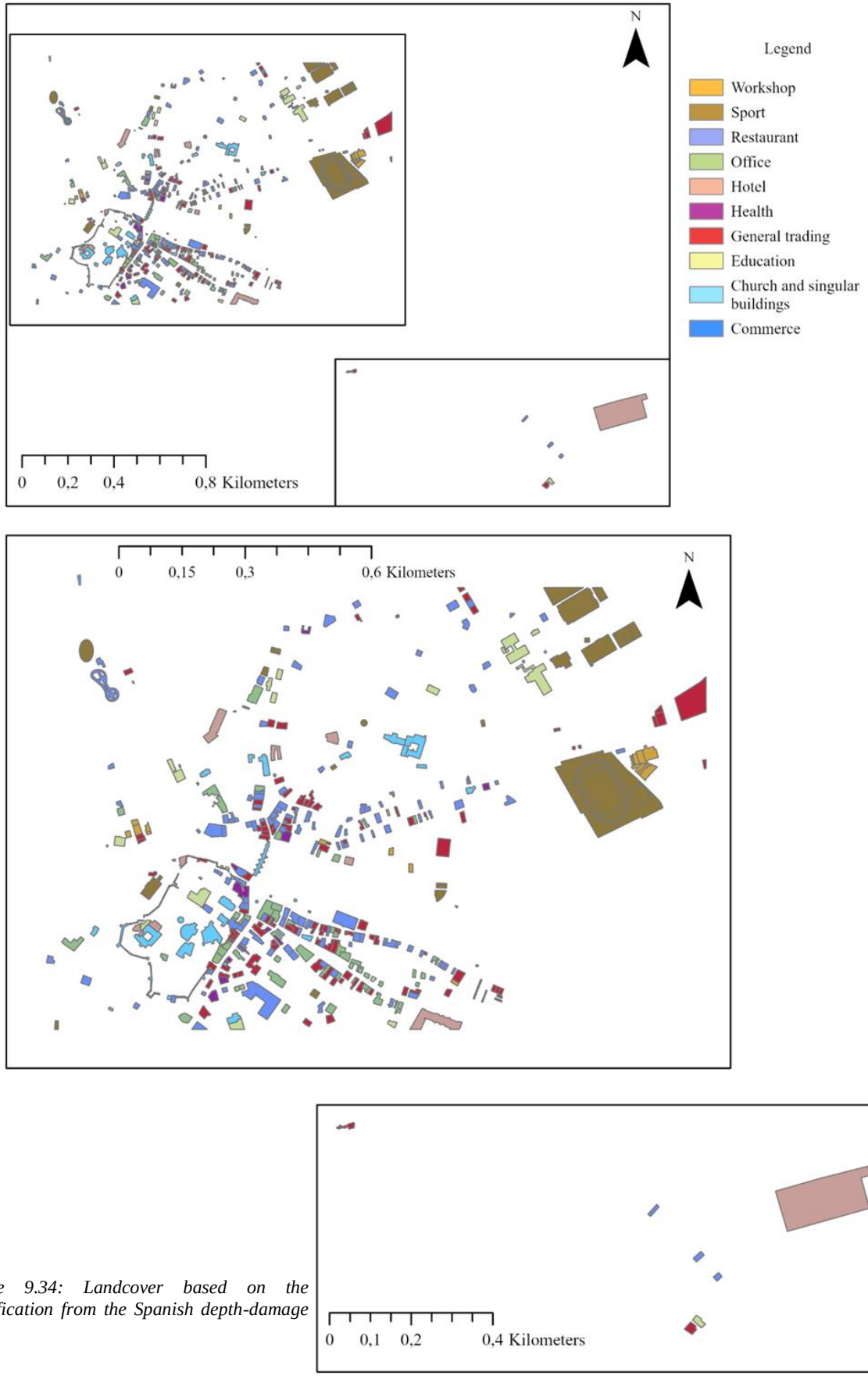

Figure 9.34: Landcover based on the classification from the Spanish depth-damage curve.

Appendix C- Probability-damage curves for the mid and long term development

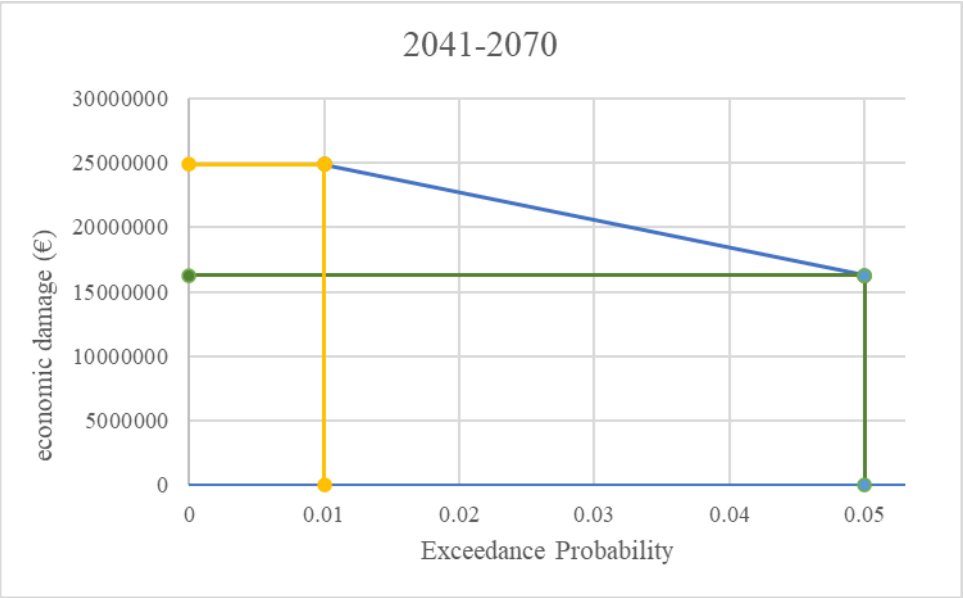

Figure 9.35: Probability-damage curve for the mid term development.

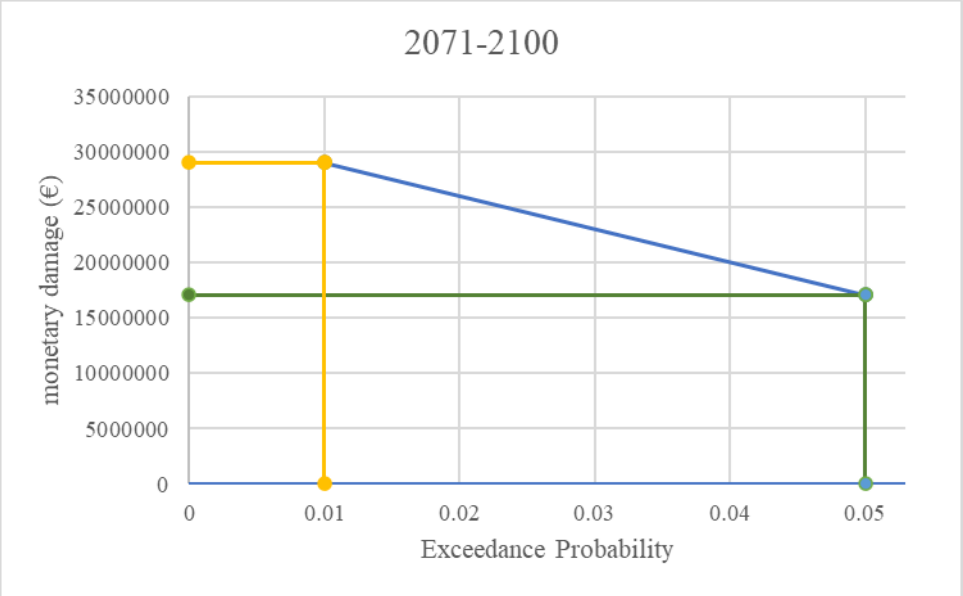

Figure 9.36: Probability-damage curve for the long term development.

Appendix D- Risk maps for the mid and long term development

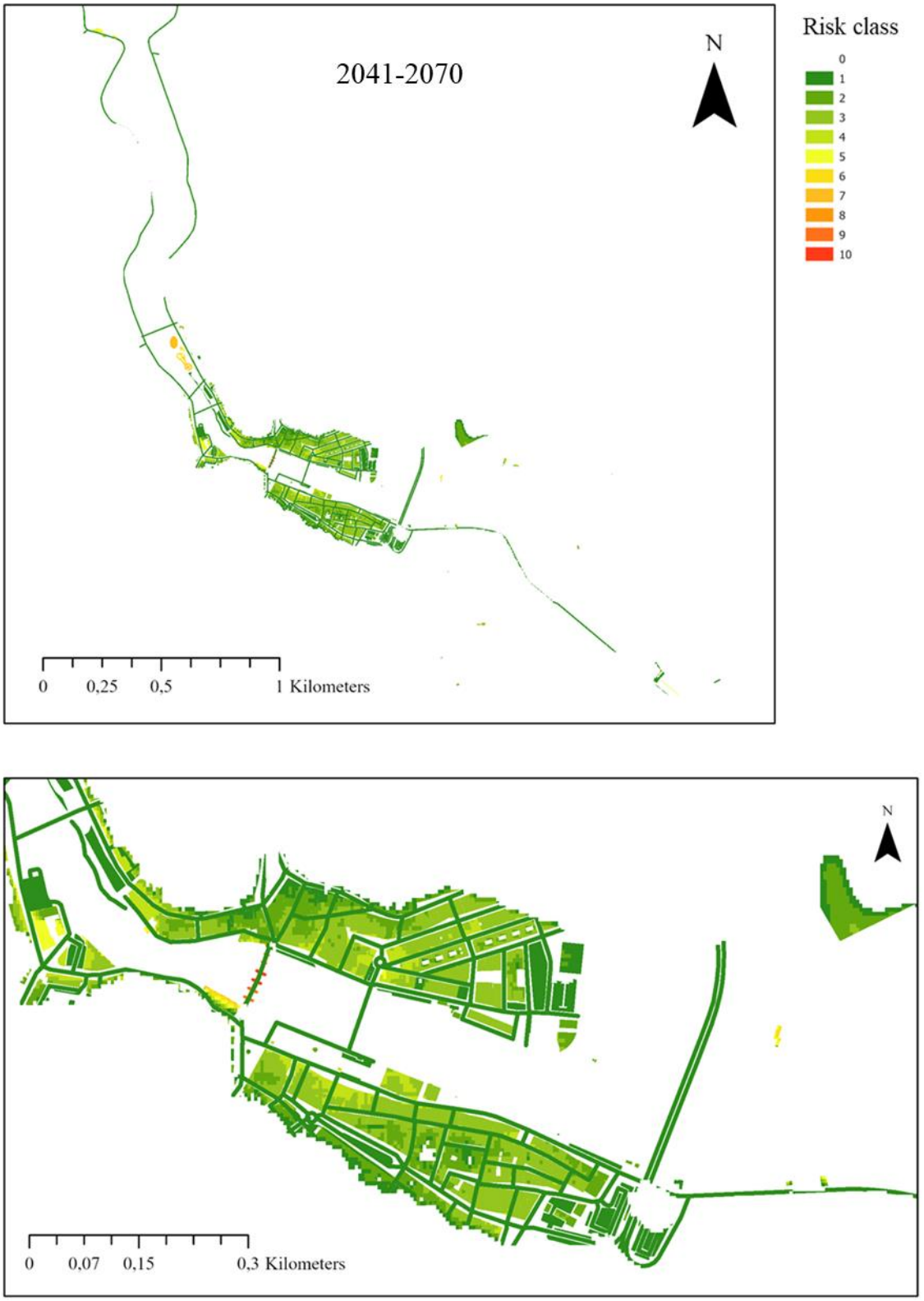

Figure 9.37: Economic risk map for the mid term development.

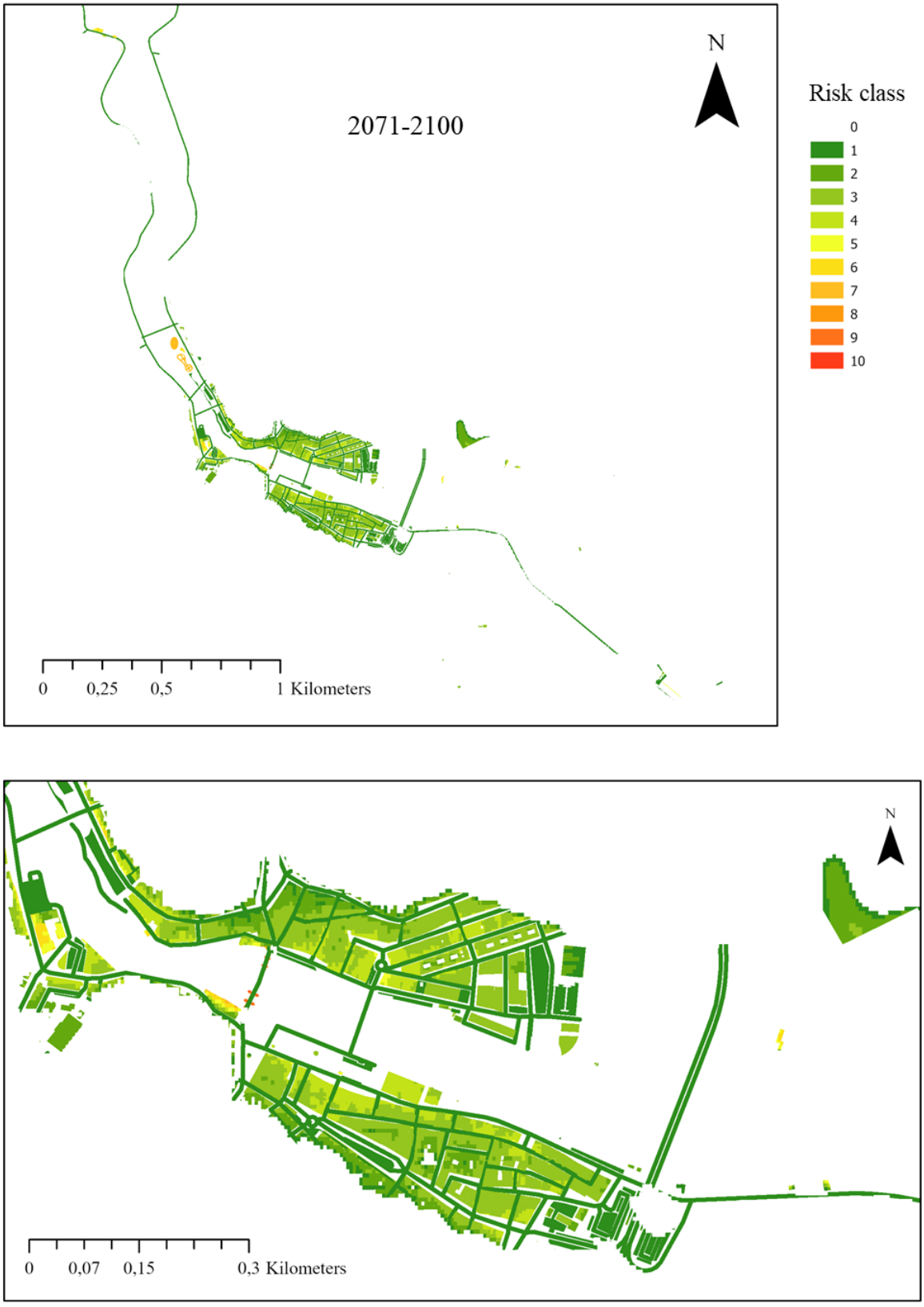

Figure 9.38: Economic risk map for the long term development.

Appendix E- Land use maps of the study area of the years 1990, 2000, 2006, 2012, and 2018

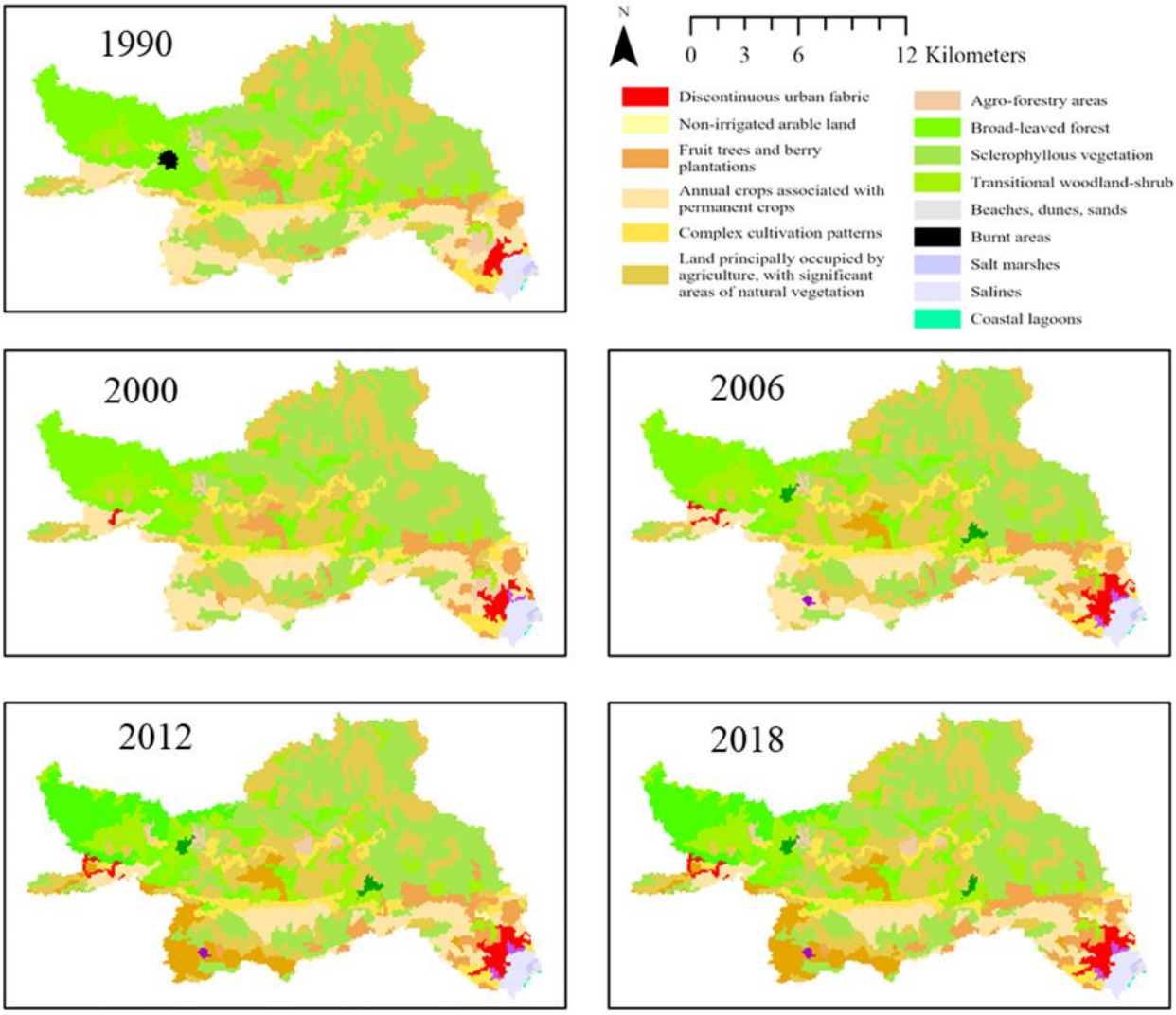

Figure 9.39: Land use maps of the study area of the years 1990, 2000, 2006, 2012, and 2018